Colloquium: Time-reversal violation with quantum-entangled B mesons

J. Bernabéu[1, a)] and F. Martínez-Vidal[1, b)]

IFIC, Universitat de València-CSIC, E-46071 València, Spain

(Dated: 8 October 2014)

Symmetry transformations have been proven a bedrock tool for understanding the nature of particle interactions, formulating and testing fundamental theories. Based on the up to now unbroken CPT symmetry, the violation of the CP symmetry between matter and antimatter by weak interactions, discovered in the decay of kaons in 1964 and observed more recently in 2001 in B mesons, strongly suggests that the behavior of these particles under weak interactions must also be asymmetric under time reversal T. However, until the recent years there has not been a direct detection of the expected time-reversal violation in the time evolution of any system. This Colloquium examines the field of time-reversal symmetry breaking in the fundamental laws of physics. For transitions, its observation requires an asymmetry with exchange of initial and final states. We discuss the conceptual basis for such an exchange with unstable particles, using the quantum properties of Einstein-Podolsky-Rosen (EPR) entanglement available at B meson factories combined with the decay as a filtering measurement. The method allows a clear-cut separation of different transitions between flavor and CP eigenstates in the decay of neutral B mesons. These ideas have been implemented for the experiment by the *BABAR* Collaboration at SLAC's B factory. The results, presented in 2012, prove beyond any doubt the violation of time-reversal invariance in the time evolution between these two states of the neutral B meson.

PACS numbers: 13.25.Hw,11.30.Er,14.40.Nd

Keywords: Time reversal, Entanglement, Discrete and finite symmetries, CP violation, B mesons, B factories

CONTENTS

a)Also at Department of Theoretical Physics, Universitat de València, E-46100 Burjassot, Spain; Electronic mail: Jose.Bernabeu@uv.es.

b)Electronic mail: Fernando.Martinez@ific.uv.es.

I. INTRODUCTION

In particle physics not all processes are expected to run in the same way with time in one sense as they do in the opposite sense, a symmetry transformation known as time reversal T. The direct observation of this phenomenon in neutral B mesons was reported by the *BABAR* Collaboration at SLAC in November 2012[1], and was echoed in other journals and magazines[2–7]. The so-called CPT theorem, applicable to phenomena described by a local quantum field theory with Lorentz invariance and Hermiticity, implies that the CP violation observed in 1964 with neutral kaons[8,9] and in 2001 with neutral B mesons[10,11] should also reveal independently a T violation for those systems. Why 48 years after the discovery of CP violation? The conceptual basis for solving the problem of how to probe time reversal with unstable systems was proposed[12–14] in 1999 through the Einstein-Podolsky-Rosen (EPR) quantum entanglement of the two neutral B mesons produced at the so-called B factories, in addition to using their two decays as filtering measurements to project definite states of the neutral B meson. In this Colloquium we review the fundamentals of time-reversal symmetry, its implication for transitions between two quantum states of the neutral B meson, the implementation of genuine T asymmetries by means of specific decay channels, and the experimental analysis leading to the direct detection performed by *BABAR* at a significance of 14σ.

The outline of the article is as follows. We first introduce the basics of time-reversal physics, presenting briefly the role of the time-reversal symmetry in the fundamental laws of classical and quantum mechanics, the different scenarios to search for T violation and to prove

it experimentally, in particular when considering unstable systems. In Sec. III we introduce the B factories and discuss how the quantum entanglement in decays of the $\Upsilon(4S)$ resonance has been employed during the last decade to perform flavor tagging for exploring CP violation in neutral B mesons. Section IV discusses how the lack of definite states of the two mesons in the entangled system before their decay can lead to either flavor tagging or "CP tagging" for the preparation of neutral B meson states required to directly test time-reversal symmetry. Section V briefly presents the $BABAR$ detector and data sample, describes how the time-reversal physics is extracted from the data, and summarizes the results and their interpretation. We conclude and discuss some perspectives in Sec. VI.

II. TIME-REVERSAL SYMMETRY IN PHYSICS

Time enters at the most elementary level as a parameter in the description of physical phenomena, serving to identify the order of a sequence of events in the evolution of a physical system. Quantitatively it can be constructed in terms of a well established and continuing sequence of repetitive events. If the period of repetition is constant it may be used as a unit of time. An accurate definition of this unit is a prerequisite to reach a good precision in time measurements to observe the details of the evolution.

The symmetry transformation that changes a physical system with a given sense of the time evolution into another with the opposite sense is called time reversal T. It corresponds to changing the sign of the velocity vector $\mathbf{v}$ or the momentum $\mathbf{p}$, without changing the position $\mathbf{r}$. In the dynamical equations of motions, or their solutions, such a transformation corresponds formally to replacing t by $-t$. The T transformation changes the sign of other dynamical variables such as angular momentum. For fields, the magnetic field changes its sign under time reversal, whereas the electric field does not.

A. Classical and quantum mechanics

The time-reversal transformation in classical mechanics corresponds to substitute for each trajectory $\mathbf{r}(t)$ the trajectory $\mathbf{r}(-t)$, i.e. to moving along the given trajectory with the opposite velocity at each point, as illustrated in Fig. 1. It is not obvious that the dynamics remains invariant under this T transformation. If the original trajectory is dynamically possible, $d\mathbf{p}/dt = \mathbf{F}$ with a force $\mathbf{F}$ depending on the sense (sign) of the velocity leads to a violation of T invariance.

In quantum mechanics, Wigner's time-reversal transformation[15],

$$\psi(t) \xrightarrow{T} \psi(t) \equiv \psi_T(t) = \psi^*(-t), \qquad (1)$$
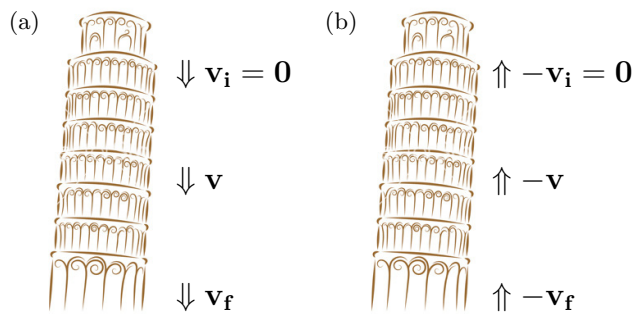

FIG. 1. (a) Trajectory of a stone falling from the leaning tower. (b) Trajectory after time-reversal transformation.

keeps the Schrödinger equation, $i\hbar\partial\psi(t)/\partial t = \mathcal{H}\psi(t)$, invariant under a T transformation if the Hamiltonian $\mathcal{H}$ is real. This has three fundamental consequences[16–19]. First, the T operator is antiunitary. This property can be seen, for example, evaluating the scalar product of two states,

$$\langle\psi_T(t)|\phi_T(t)\rangle = \langle\psi(-t)|\phi(-t)\rangle^* = \langle\phi(-t)|\psi(-t)\rangle. \quad (2)$$

Thus, time reversal has to do with interchange of bra and ket states. Second, the complex conjugation implies that time reversal does not have observable and conserved eigenvalues, unless $\psi(t)$ is purely real. Third, for a plane wave with momentum $\mathbf{p}$, $\psi(\mathbf{r},t) = \exp[i(\mathbf{p}\cdot\mathbf{r} - Et)/\hbar]$, the time-reversed wavefunction is $\psi^*(\mathbf{r},-t) = \exp[i(-\mathbf{p}\cdot\mathbf{r} - Et)/\hbar]$, i.e. the T-transformed function describes a particle with momentum $-\mathbf{p}$ and energy E, thus it is not necessary to interpret the transformed function as a particle going backwards in time. For this reason the T transformation is often referred to as "motion reversal" rather than "time reversal".

The T transformation is implemented in the space of states by the antiunitary operator U_T in such a way that, for spinless particles,

$$U_T\mathbf{r}U_T^\dagger = \mathbf{r}, \ U_T\mathbf{p}U_T^\dagger = -\mathbf{p}, \qquad (3)$$

and $\psi_T(t) = U_T\psi(-t)$. Equation (3) guarantees the invariance of the commutation rule between $\mathbf{r}$ and $\mathbf{p}$, thus we might say that T transforms quantum mechanics into quantum mechanics. For a Hamiltonian $\mathcal{H}$ invariant under time reversal, $[\mathcal{H}, U_T] = 0$, the time-evolution operator $\mathcal{U}(t, t_0)$ transforms as

$$U_T\mathcal{U}(t, t_0)U_T^\dagger = \mathcal{U}^\dagger(t, t_0). \qquad (4)$$

The antiunitary character of U_T allows to write $U_T = UK$, where U is unitary ($U^{-1} = U^\dagger$) and K is an operator which complex conjugates all complex numbers. For the matrix elements of time-dependent transitions we have

$$\langle f|\mathcal{U}(t, t_0)|i\rangle = \langle f|U_T^\dagger U_T\mathcal{U}(t, t_0)U_T^\dagger U_T|i\rangle$$
$$= \langle U_T f|\mathcal{U}^\dagger(t, t_0)|U_T i\rangle^* = \langle U_T i|\mathcal{U}(t, t_0)|U_T f\rangle, \quad (5)$$

where time-reversal invariance is assumed when passing from the first to the second lines of Eq. (5). As a consequence, the comparison between $i \to f$ and $U_T f \to U_T i$ transitions is a genuine test of this invariance. It is because of these special properties that the role of time reversal is distinct from that of any other symmetry operation in physics, and makes its experimental investigation significantly more difficult than other symmetries.

Therefore, time-reversal in classical mechanics as well as in quantum mechanics is related to the following fundamental question (see Fig. 1): consider a point over a trajectory (a state in quantum mechanics), invert the velocities of all particles in that point, and let it evolve; shall we obtain the former initial point of the trajectory with all velocities reversed? Obviously, for a fair comparison the experiment should be repeated in the laboratory with exactly the same boundary conditions as in the T mirror, since the motion is not only determined by the equations of motion but also by the boundary conditions, and the symmetries of the motion cannot be greater than those of the latter. From Newton's mechanics to electrodynamics, the dynamical laws of physics are symmetric under T transformation.

Motion-reversal symmetry implies, for a given configuration of energy-momenta and spin, the reciprocity relation[16–19]: the probability of an initial state i being transformed into a final state f is the same as the probability that an initial state identical to f, but with momenta $\mathbf{p}$ and spins $\mathbf{s}$ reversed, transforms into the state i with momenta and spins reversed,

$$|\langle f|\mathcal{S}|i\rangle|^2 = |\langle U_T i|\mathcal{S}|U_T f\rangle|^2, \qquad (6)$$

where $\mathcal{S}$ is the transition matrix determined by the Hamiltonian $\mathcal{H}$. Here, $|i\rangle \equiv |\mathbf{p}_i, \mathbf{s}_i\rangle$ and $\langle f| \equiv \langle \mathbf{p}_f, \mathbf{s}_f|$ are the initial and final states, $\langle U_T i|$ and $|U_T f\rangle$ are the transformed states of $|i\rangle$ and $\langle f|$, respectively, $\langle U_T i| \equiv \langle -\mathbf{p}_i, -\mathbf{s}_i|$ and $|U_T f\rangle \equiv |-\mathbf{p}_f, -\mathbf{s}_f\rangle$. It should be noted that T invariance is a sufficient, but not necessary, condition for Eq. (6). Therefore, a breaking of reciprocity is an unambiguous signal for T violation. If $\mathcal{S}$ is Hermitian, $|\langle f|\mathcal{S}|i\rangle| = |\langle U_T i|\mathcal{S}|U_T f\rangle| = |\langle U_T f|\mathcal{S}|U_T i\rangle|$; in this case, T invariance implies T-odd invariance, and vice versa, where the T-odd transformation only refers to changing the sign of all odd variables under $t \to -t$ in $\mathcal{H}$, without exchanging initial and final states. This occurs, for instance, to first order in weak interactions when final state interactions (FSI) can be neglected[19].

The reciprocity relation establishes a connection between the differential cross-sections for reactions $a+b \to c+d$ and $c+d \to a+b$ (detailed balance). It has been verified by experiment in nuclear reactions due to strong or weaker interactions, for example[20]

$$\alpha(0^+) + {}^{24}\text{Mg}(0^+) \to {}^{27}\text{Al}(5/2^+) + p(1/2^+). \qquad (7)$$

Here, if is there any T violation it cannot exceed a half per mil.

B. Complex systems and the arrow of time

When discussing T violation we should clearly distinguish t asymmetry of complex systems. For example, our daily experience shows us that when a vase falls and breaks into pieces it is not possible that the pieces of the group fly back in reverse order, forming the vase. This macroscopic t asymmetry, also known as "arrow of time", is in the nature of thermodynamics. As discussed by Eddington[21], the arrow of time is a property of entropy alone, a measurement of disorder: the arrow gives the direction of progressive increase of disorder in isolated systems. How it is then possible to generate thermodynamic irreversibility from fundamental laws that are T symmetric? The answer to this question is that the thermodynamic irreversibility is associated to the irreversibility of the initial conditions for systems with large number of degrees of freedom, larger for more disordered states, making very unlikely (although not forbidden) for a system to evolve from a disordered to a more ordered state. In the example of the falling vase, with $\mathcal{O}(10^{24})$ of particles and collisions, it is not possible in practice to set up the initial conditions for the reversed process (positions and velocities).

There is no doubt that the Universe is expanding, even accelerating at the present times, thus we have a time-asymmetric behavior. But this Universe t asymmetry is perfectly compatible with T-symmetric laws of physics. If we think of the initial condition of our Universe (likely inflation[22–25]) as an improbable state, i.e. more ordered, the cosmological t asymmetry is probably connected with the arrow of time for complex systems. However, none of these time asymmetries is fundamental T violation.

In particle physics, as will be discussed further in detail in Sec. II E, decays are an example of thermodynamically asymmetric processes: the number of variables or degrees of freedom describing the final state is larger than the number of variables needed to describe the initial state.

C. Discrete symmetries broken by weak interactions

It is well known since 1957 that weak interactions have little respect for symmetries. That year space inversion (parity, P) symmetry was discovered to be broken in beta decays[26–28]. Then, there was the hope that the combination of P with charge conjugation (CP) was a good symmetry. But just a few years later, in 1964, there was discovered a small but unambiguous violation of the CP symmetry in K meson decays[8,9]. More recently, in 2001, the B factory experiments BABAR and Belle, observed that CP is violated in B mesons[10,11].

The now well established CP violation in the quark sector can be successfully accommodated within the Standard Model (SM) of particles and fields through the three-family Cabibbo-Kobayashi-Maskawa (CKM) quark-mixing mechanism[29,30]. It describes the coupling of the W boson to up and down quarks and conveys
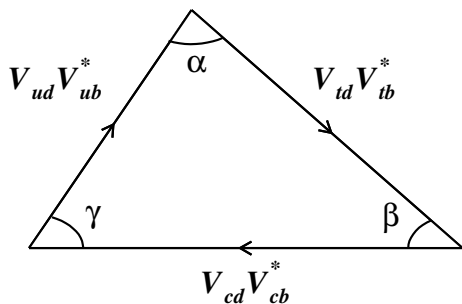
FIG. 2. The bd unitarity triangle representing the CKM unitarity conditions. The three sides are determined from semileptonic and non-leptonic B decays, including B^0-$\bar{B}^0$ oscillations. Since they are of comparable length the angles are sizeable and one expects large CP asymmetries in B decays in the SM. There are other two triangles which almost collapse to a line. This gives an intuitive understanding of why CP violation is small in the leading K decays (ds triangle) and in the leading B_s decays (bs triangle).

the fact that the quarks with definite properties under charged-current weak interactions are linear combinations of the quark mass eigenstates[31]. For three families, the unitarity conditions of the quark-mixing matrix V are represented by triangles in the complex plane, as illustrated in Fig. 2, and lead to four fundamental parameters: three magnitudes and one single irreducible phase. In the Wolfenstein parameterization[32] we can write to $\mathcal{O}(\lambda_c^4)$ as

$$
\begin{bmatrix} V_{uj} \\ V_{cj} \\ V_{tj} \end{bmatrix} = \begin{bmatrix} 1 - \lambda_c^2 & \lambda_c & A\lambda_c^3(\rho - i\eta) \\ -\lambda_c & 1 - \lambda_c^2/2 & A\lambda_c^2 \\ A\lambda_c^3(1 - \rho - i\eta) & -A\lambda_c^2 & 1 \end{bmatrix},
$$

where the index j runs over d, s, and b quarks, and $\lambda_c \approx 0.226$, $A \approx 0.814$, $\rho \approx 0.135$ and $\eta \approx 0.349$[31]. Extensive tests of the CKM mechanism using all experimental data show a high degree of consistency[33]. Historically, Kobayashi and Maskawa extended in 1973 the 2×2 Cabibbo mixing matrix to 3×3 to explain the CP violation discovered nine years before, thus anticipating the existence of the third family of quarks, quickly confirmed with the discovery of the τ lepton in 1975[34] and of the fifth quark, the b, two years later[35].

All local quantum field theories with Lorentz invariance and Hermiticity respect CPT symmetry[36,37], in accordance with all experimental evidence[31], hence there is a straightforward theoretical connection between CP and T violation (matter-antimatter asymmetry defines a preferred sense of time evolution). Since the SM is based on a quantum field theory satisfying the CPT theorem, it follows that the source of CP violation also requires

of T-violating effects. With the complex Hermitian Lagrangian, genuine CP phases change sign for particles and antiparticles, so its experimental detection requires an interference experiment to observe the relative CP phase between the interfering complex amplitudes. Therefore, given the known CP violation in weak interactions in processes involving K and B mesons, T should also be broken in these systems. The question is whether the expected T asymmetry can be detected by an experiment that, considered by itself, clearly shows a motion-reversal asymmetry independent of CP asymmetries and CPT invariance.

D. Experiments probing T violation

There are two main types of experiments or observables that can be used to detect directly time-reversal non-invariance[14,16,17].

A non-zero expectation value of a T-odd operator for a non-degenerate stationary state. This is the case for an electric dipole moment (e.d.m.) of a particle with spin, which is also a P-odd, C-even quantity, as depicted in Fig. 3. A parity transformation about the midplane of the sphere flips the e.d.m. $\boldsymbol{d}$ with respect to the magnetic dipole moment $\boldsymbol{\mu}$ (spin), which remains unchanged, whereas a time-reversal transformation flips $\boldsymbol{\mu}$ with respect to $\boldsymbol{d}$, which is in this case unaffected. Thus, if either parity or time reversal are good symmetries, the particle cannot have an e.d.m. since one can distinguish the mirror picture from the original one. A non-zero e.d.m. can be generated by either strong T violation unless it is annulled by a Peccei-Quinn symmetry leaving the axion as remnant[38], or by T violation in weak interactions. In the SM with the CKM mechanism, a non-vanishing e.d.m. of the neutron only appears at three-loop level. Hence, these experiments probe for physics beyond the SM. To date, no signals for e.d.m. have been found, although there are strong limits, as for the neutron and the electron, $|\boldsymbol{d}_n| < 2.9 \times 10^{-26}$ e- cm and $|\boldsymbol{d}_e| < 1.05 \times 10^{-27}$ e-cm[31].

Experiments involving T-odd observables for weak decays (as well as electromagnetic transitions), constructed typically using odd products of the momentum and spin vectors of the decay products (initial and final states), are sometimes used. These observables are not genuine signals for T violation since initial and final states are not interchanged, and in general require detailed understanding of FSI effects since they can mimic T violation even with time-reversal symmetric dynamics[14,17,31]. In some cases, T-odd CP asymmetries can be built by comparing particle and antiparticle decays, without knowing the CP-even FSI phases (see for example[39] and references therein).

We might also consider transition processes. As discussed before and illustrated in Fig. 4, the antiunitary character of the T operator demands the exchange of initial and final states to compare the probabilities
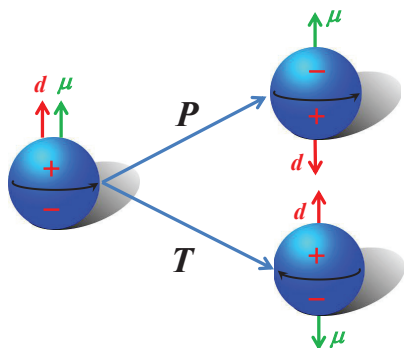
FIG. 3. A particle with spin is represented as a sphere with a spinning charge distribution. Its parity and time-reversed images are also shown, together with the corresponding magnetic $\boldsymbol{\mu}$ and electric $\boldsymbol{d}$ dipole moments.

$|\langle f|\mathcal{U}(t,t_0)|i\rangle|^2$ and $|\langle U_T i|\mathcal{U}(t,t_0)|U_T f\rangle|^2$, once the initial conditions, namely i in one case and $U_T f$ in the other, have been precisely realized. With stable particles one can consider neutrino ν_e to ν_μ mixing[40], but this requires high-luminosity and long-baseline neutrino facilities. Alternatively, neutral K and B mesons, the unique systems for which CP violation has been detected, are a best choice for an experiment probing T non-invariance. Nevertheless, the thermodynamic irreversibility of these systems makes this option difficult, as discussed below.
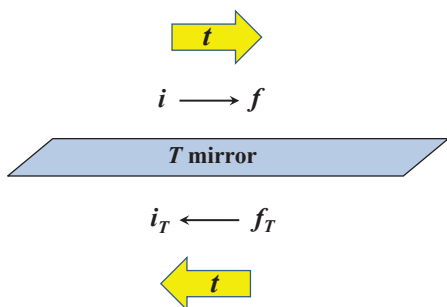

FIG. 4. The antiunitary property of the T operator demands the exchange of initial and final states to set up an experiment directly probing time-reversal symmetry in transitions. Motion-reversal symmetry implies equal probabilities for transitions $i \to f$ and $i_T \leftarrow f_T$, once the initial conditions, namely i in one case and f_T in the other, have been precisely realized. Here, i_T and f_T are the T-transformed states of i and f, respectively, with all momenta and spins reversed.

E. Unstable systems

A direct consequence of quantum dynamics is the negative-exponential time behavior of the decay of any unstable system into two or more particles, as given by the Fermi golden rule. The reversal of the exponential decay law reveals that the T transformation is not defined for a decaying state, thus it appears that the decay prevents proofs of motion reversal. This apparent imbalance in time has to do with initial conditions rather than with the dynamics under time reversal; we have assumed that the initial system is the unstable particle, but it should be formed by some process before. Hence, to address the question of time reversal we have to choose an initial time earlier so that the production enters into the process[17].
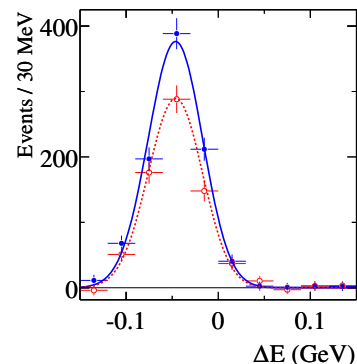

FIG. 5. Energy distributions of $B^0 \to K^+\pi^-$ (solid circles and solid curve) and $\bar{B}^0 \to K^-\pi^+$ (open circles and dashed curve) decays[41]. Points with error bars are data and the curves are best fit projections. The difference between the two distributions is a signature of direct CP violation.

For example, we might consider the decay of a neutral B meson into the final state $K^+\pi^-$, i.e. $B^0 \to K^+\pi^-$, with rate R_1. CP violation is known to be large in this decay[41,42], thus we have $\bar{B}^0 \to K^-\pi^+$ with rate $R_2 \neq R_1$, as can be observed in Fig. 5. In the SM, this decay occurs through two different amplitudes (penguin and tree), with different weak phases and, in general, different strong phases. This is a general requirement[43] to generate a non-vanishing interference for particle and antiparticle decays[44]. This leads to a difference in the decay rates for CP conjugate processes, which we refer to as direct CP violation. The B meson production could be done in electron-positron annihilation reactions through the process $e^+e^- \to \Upsilon(4S) \to B^0\bar{B}^0$ at a center-of-mass energy (c.m.) of 10.58 GeV. Here only one of the produced neutral B mesons is analyzed for its decay into $K^+\pi^-$ or $K^-\pi^+$, whereas the other is not studied and might decay into any final state, say $\bar{B}^0 \to \bar{X}$ or $B^0 \to X$. By CPT invariance the time-reversed processes, $K^+\pi^- \to B^0$ and $K^-\pi^+ \to \bar{B}^0$,

would have expected rates R_1 and R_2, respectively. However, the experiment probing motion reversal should form the two B mesons and the $\Upsilon(4S)$, through the chain reactions $(K^+\pi^- \to B^0)(\overline{X} \to \overline{B}^0) \to \Upsilon(4S)$ and $(K^-\pi^+ \to \overline{B}^0)(X \to B^0) \to \Upsilon(4S)$. This is clearly a problem of thermodynamic irreversibility. Besides, even if we could build such a set up, strong interaction processes in the kaon-pion annihilation would completely swamp the weak interaction process responsible for the decay.

We might consider motion reversal in the mixing, often also referred as oscillation, of the pseudoscalar neutral K, B and D mesons. In this case one compares the probability of a flavor eigenstate (say) K^0 transforming into a $\overline{K}^0$, and vice versa. Since the states K^0 and $\overline{K}^0$ are particle and antiparticle, the two transitions are connected by both T and CP transformations. Even if CPT symmetry would be broken, there exists no difference between CP and T in this case. Thus the two symmetry transformations are experimentally identical and lead to the same asymmetry. This flavor-mixing or Kabir asymmetry[45] is independent of time since the two processes have identical time dependence, and is induced by the interference between the dispersive, M_{12}, and absorptive, Γ_{12}, contributions to the mixing of K^0 and $\overline{K}^0$ states. Here, M and Γ are the 2×2 mass and decay Hermitian matrices of the effective Hamiltonian describing neutral meson mixing, $\mathcal{H}_{\text{eff}} = M - i\Gamma/2$[19,46], and the index 1 (2) refers to B^0 ($\overline{B}^0$) state.

Evidence at 4σ level for this asymmetry was found by the CPLEAR experiment at CERN in 1998 by studying the reaction $p\bar{p} \to K^\pm\pi^\mp K^0(\overline{K}^0)$ in $p\bar{p}$ collisions[47]. The strangeness (strange and antistrange flavor content) of the K^0 and $\overline{K}^0$ mesons at production time was determined by the charge of the accompanying charged kaon. Since weak interactions do not conserve strangeness, the K^0 and $\overline{K}^0$ may subsequently transform into each other. The strangeness of the neutral kaon at decay time is determined through the semileptonic decays $K^0 \to e^+\pi^-\nu_e$ and $\overline{K}^0 \to e^-\pi^+\bar{\nu}_e$, respectively. The asymmetry, shown in Fig. 6, is effectively independent of time, and reveals a net offset with respect to zero.

The interpretation of the asymmetry relies on two main aspects. Firstly, in the framework of the Weisskopf-Wigner approach[48,49], the effect comes from the overlap (non-orthogonality) of the "stationary" K_S^0 and K_L^0 physical states. Secondly, the decay plays an essential role; indeed, within the SM the dispersive and absorptive contributions to K^0-$\overline{K}^0$ mixing (Fig. 7) are at leading order proportional to the mass and decay width differences between the K^0 and $\overline{K}^0$ mass eigenstates[19,31], respectively. The presence of the decay as an initial state interaction, essential to construct a non-vanishing interference for this observable, has been argued by Wolfenstein to claim that this asymmetry "is not as direct a test of time-reversal violation as one might like"[14,50]. In the neutral B system, where the decay width difference between the B^0 and $\overline{B}^0$ mass eigenstates is negligible, the measurement of this
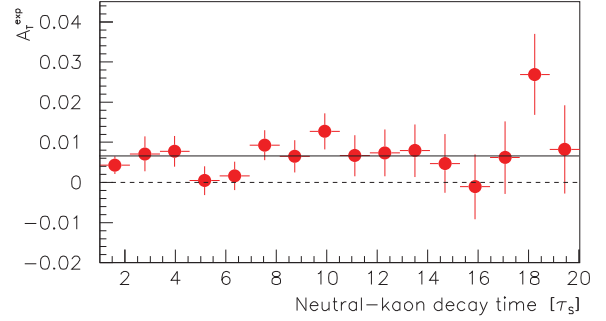

FIG. 6. The CPLEAR asymmetry versus the neutral-kaon decay time (in units of the K_S^0 lifetime)[47]. The solid line represents the average.

asymmetry has, in fact, brought negative results[51–54]. Other authors, however, have argued that its interpretation as a genuine signal for T violation does not get affected by these arguments[55–57].
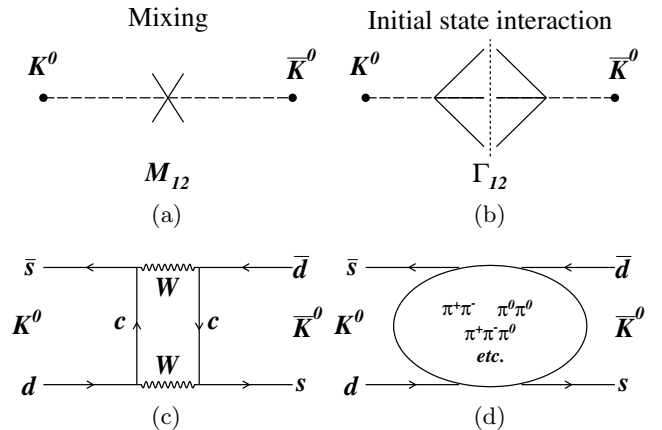

FIG. 7. The $K^0 \to \overline{K}^0$ versus $\overline{K}^0 \to K^0$ mixing asymmetry arises from the interference between the dispersive (a) and absorptive (b) contributions to K^0-$\overline{K}^0$ mixing. Diagram (a) involves short-distance box diagrams (c) as well as long-range interactions (d) in which the intermediate states are off-shell mesons. The box diagram is matched by another where the quark triplet and the W bosons are interchanged. Diagram (b) is referred to as "initial state interaction" since it involves decay to intermediate on-shell states (d), and it is proportional to the decay width difference between the K^0 and $\overline{K}^0$ mass eigenstates.

III. B FACTORIES AND CP VIOLATION

At the asymmetric B factories, electron and positron beams collide with high luminosity at a c.m. energy of 10.58 GeVcorresponding to the mass of the $\Upsilon(4S)$ resonance, a vector particle with $J^{PC} = 1^{--}$. The $\Upsilon(4S)$ is abound state of a b and a $\overline{b}$ quark, that decays exclusively to a pair of B and $\overline{B}$ mesons. Since the mass of the $\Upsilon(4S)$ is only slightly higher than twice the mass of the B meson, the two B mesons have low momenta (about 330 MeV/c) and are produced almost at rest in the $\Upsilon(4S)$ reference frame with no additional particles besides those associated to the B decays. The energy of the electron beam is adjusted to be between twice and three times larger than that of the positrons, so that the c.m.frame has a Lorentz boost along the collision axis. Two B factory colliders, PEP-II at SLAC in California and KEKB at KEK in Japan, with their corresponding detectors, $B\!A\!B\!A\!R$[58,59] and Belle[60], have been operating during the last decade, accumulating an integrated luminosity of data exceeding 500 fb^{-1} and 1 ab^{-1}, respectively.

The electron- and positron-beam energies have been designed to be 9.0 and 3.1 GeV at PEP-II, and 8.0 and 3.5 GeV at KEKB, thus the Lorentz boosts $\beta\gamma$ are about 0.56 and 0.42, respectively. This allows a mean separation of the two B mesons along the collision axis in the laboratory frame of about 250 and 200 μm. With a typical detector resolution of 100 μm, it is possible to experimentally determine the distance Δz between the decay points of the two Bs to obtain the decay time difference $\Delta t \approx \Delta z/(\beta\gamma c)$. This translates into a mean time separation of about 1.5 ps with a resolution ranging typically between 0.6 and 0.8 ps.

A. Entangled neutral B mesons

The decay of the $\Upsilon(4S)$ particle occurs through strong interactions, thus the system of the created pair of B and $\overline{B}$ mesons inherits the $\Upsilon(4S)$ quantum numbers. About 50% of the $B\overline{B}$ pairs are $B^0\overline{B}^0$, when the hadronization process pick ups a $d\overline{d}$ quark pair, and 50% B^+B^- when it is a $u\overline{u}$ pair.

Because B and $\overline{B}$ are two pseudoscalar states of a unique (complex) field, Bose statistics and angular momentum conservation requires that the wavefunction of the $B\overline{B}$ pair be in a P-wave, antisymmetric CP-even state[61],

$$|\Upsilon\rangle = \frac{1}{\sqrt{2}} \left[|B^0(t_1)\rangle|\overline{B}^0(t_2)\rangle - |\overline{B}^0(t_1)\rangle|B^0(t_2)\rangle \right]. \quad (8)$$

The times t_1 and t_2 in Eq. (8) do not refer to time dependence but labels to characterize the states: state 1 (2) is labeled as the first (second) to decay, i.e. $t_1 < t_2$. The antisymmetric entanglement is essential: even with B^0-$\overline{B}^0$ mixing between the production time at $t = 0$ and the first decay at $t = t_1$, the state $|\Upsilon\rangle$ remains antisymmetric,

with no trace of combinations $|B^0\rangle|B^0\rangle$ or $|\overline{B}^0\rangle|\overline{B}^0\rangle$, and only $|B^0\rangle|\overline{B}^0\rangle$ and $|\overline{B}^0\rangle|B^0\rangle$ states appearing at any time. The state of the first B to decay at t_1 dictates the state of the other B, without measuring (thus destroying) it, and then evolves in time and decays at t_2. The antisymmetric wavefunction defined by this EPR entanglement[62,63] is usually written in terms of the strong-interaction flavor eigenstates B^0 and $\overline{B}^0$, as given by Eq. (8). It should be noted that the basis choice of B^0 and $\overline{B}^0$ states is only a matter of convention. The individual state of each neutral B is not defined in the entangled state $|\Upsilon\rangle$ before the first decay. The quantum collapse of the state at decay time t_1 to a flavor specific channel tags the second B as the orthogonal state.

Now, consider that the first B decays semileptonically producing a negatively-charged prompt lepton. As shown in Fig. 8, this decay proceeds through a $b \to c$ transition, and the charge of the lepton is completely correlated with the flavor of the b quark, hence the parent B is a $\overline{B}^0$ at the instant of its decay. The anticorrelation defined by the wavefunction determines that the other B at that time is a B^0, thereby it prepares (or tags) a B^0 flavor state. In quantum mechanics language this means that the initial state of the B meson has been prepared or filtered as B^0. Neutral B mesons start to oscillate just after their production since their mixing rate, $\Delta m_d \approx 0.5$ ps^{-1}, is comparable to their decay width, $\Gamma_d \approx 0.7$ ps^{-1}. Thus, the state prepared as B^0 will be a superposition of B^0 and $\overline{B}^0$ at a later time. As will be discussed further in Secs III B and IV, this quantum mechanical superposition of states is of key importance for the experimental exploration of CP and, especially, time-reversal symmetries. Analogously, with a positively-charged prompt lepton we would have a $\overline{B}^0$ tag. There are other signatures that can be used, like prompt charged kaons produced through a $b \to c \to s$ cascade, as sketched in Fig. 8. In the following, we denote generically as $\ell^- \overline{X}$ or $\ell^+ X$ any flavor-specific final state that can be used to identify the flavor of the decaying B. Note that for this procedure to work only right-sign decays should take place, i.e. the wrong-sign decays $B^0 \to \ell^- \overline{X}$ and $\overline{B}^0 \to \ell^+ X$ do not occur.

B. CP violation at B factories

Flavor tagging based on quantum entanglement has been the basis for a decade of CP violation physics at B factories. In these studies, the second B meson, the one that is not used for flavor tagging, is reconstructed into a CP-eigenstate final state, for example $J/\psi K_s^0$, which has CP-odd parity (except for 0.1% due to CP violation in K^0-$\overline{K}^0$ mixing[31]). The decay of the B meson into the flavor-eigenstate final state can occur after the decay into the CP eigenstate; to account for this situation the experiments define as convention a signed decay time difference,

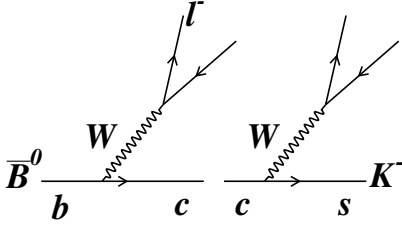$$\Delta t = t_{CP} - t_{\text{flavor}}. \quad (9)$$

FIG. 8. A $\bar{B}^0$ meson, containing a b quark, decays dominantly with lifetime ~ 1.5 ps through a $b \to c$ transition. The virtual W^- gauge boson creates a negatively-charged prompt lepton whose electric charge can be correlated with the b quark flavor. The charge of kaons produced through the $b \to c \to s$ cascade also identifies the flavor of the B meson.

CP violation means any difference between the decay rate $B^0 \to J/\psi K_s^0$ and its CP conjugate, $\bar{B}^0 \to J/\psi K_s^0$. The search for this asymmetry has been the raison d'être of the B factories. Experimentally everything is identical for the two processes, except the requirement of a $\ell^- \bar{X}$ or a $\ell^+ X$ decay of the B meson used for tagging. The large CP violation observed by the B factory experiments in 2001[10,11] follows from the comparison of the B^0 and $\bar{B}^0$ decay rates at equal decay proper-time difference, as shown in Fig. 9(a). The difference between these two distributions signals CP violation. This is more evident in the time-dependent CP asymmetry, shown in Fig. 9(b), where the difference between the two distributions is normalized to their sum,

$$A_{CP,f} = \frac{\Gamma_{\bar{B}^0 \to f}(\Delta t) - \Gamma_{B^0 \to f}(\Delta t)}{\Gamma_{\bar{B}^0 \to f}(\Delta t) + \Gamma_{B^0 \to f}(\Delta t)}. \qquad (10)$$

It should be noted that the notion of flavor tag adopted here as preparation of the initial state of the second B, using the measurement of the decay of the first B, is different from the one commonly used by the B factory experiments, where tagging refers to the flavor identification of the first B. The reason to adopt this convention, closer to the standard quantum mechanics language, will become more clear later.

One can also use final states with different CP parity, for example the CP-even $f = J/\psi K_L^0$. Due to its opposite CP eigenvalue, the behaviors of the time distributions for B^0 and $\bar{B}^0$are interchanged and the asymmetry is opposite, as observed in Fig. 9(c,d). Besides increasing the statistical power of the result, the use of final states with opposite CP parity provides a powerful cross-check of the CP-violating effect.

This CP asymmetry is induced by the interference of amplitudes involved in the two possible paths to reach the same final state f from a B^0 (or its CP conjugate), either through decay without mixing, $B^0 \to f$, or through mixing followed by decay, $B^0 \to \bar{B}^0 \to f$. Therefore, we usually refer to CP violation in the interference between

decay amplitudes with and without mixing, or simply indirect CP violation. This type of CP symmetry breaking can be compared to direct CP violation (due to the interference of different decay amplitudes) or CP violation in mixing (arising from the interference of the dispersive and absorptive contributions to mixing)[19].
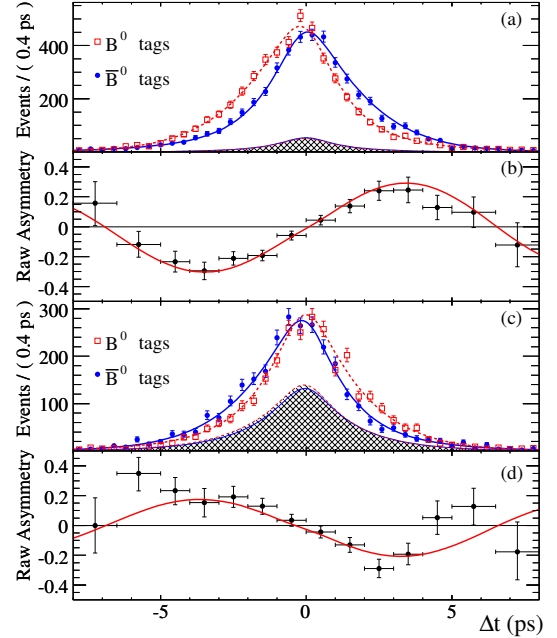

FIG. 9. Flavor-tagged Δt distributions (a,c) and CP asymmetries (b,d) from the BABAR experiment[64], for CP-odd final states $J/\psi K_s^0$, $\psi(2S)K_s^0$, $\chi_{c1}K_s^0$ and $\eta_c K_s^0$ (a,b), and the CP-even final states $J/\psi K_L^0$ (c,d). The solid (dashed) curves in (a) and (c) represent the best fit projections in Δt for $\bar{B}^0$ (B^0) tags. The shaded regions represent the estimated background contributions to (a) and (c). The curves in (b) and (d) are the fit projections of the CP asymmetry between $\bar{B}^0$ and B^0 tagged events.

The time-dependent decay rates and the CP asymmetry can be parameterized in a model-independent way, only assuming quantum mechanics, as

$$\Gamma_{\bar{B}^0(B^0) \to f} \propto e^{-\Gamma_d|\Delta t|} \times$$
$$\left\{ 1 + (-) \left[S_f \sin(\Delta m_d \Delta t) - C_f \cos(\Delta m_d \Delta t) \right] \right\}, \quad (11)$$
$$A_{CP,f} = S_f \sin(\Delta m_d \Delta t) - C_f \cos(\Delta m_d \Delta t), \qquad (12)$$

where Δm_d is the mass difference between the physical states of the neutral B meson system, and Γ_d is average total decay width. Equation (11) assumes a negligible difference between the decay rates of the mass eigenstates, i.e. $\Delta\Gamma_d = 0$, and CP symmetry in mixing (independently of whether CPT and T are or are not violated). If CP symmetry in mixing holds, then the conditions $|q/p| = 1$ and $z = 0$ apply, where q, p and z are three complex parameters introduced to define the eigenstates of well-defined mass and decay width (referred to

as mass eigenstates) in terms of the strong interaction (flavor) eigenstates[19,31]. Adopting an arbitrary sign convention[19],

$$|B_L\rangle \propto p\sqrt{1-z}|B^0\rangle - q\sqrt{1+z}|\overline{B}^0\rangle,$$
$$|B_H\rangle \propto p\sqrt{1+z}|K^0\rangle + q\sqrt{1-z}|\overline{B}^0\rangle. \quad (13)$$

Within the Weisskopf-Wigner approach, these parameters are related to the matrix elements of the 2×2 effective, non-Hermitian Hamiltonian $\mathcal{H}_{\rm eff}$ describing mixing. Note that the real and imaginary parts of the corresponding eigenvalues are the masses and decay widths, and their splittings are Δm_d and $\Delta\Gamma_d$, respectively. If either CP or CPT is a good symmetry in mixing (independent of T), then $z = 0$, and if either CP or T is a symmetry of $\mathcal{H}_{\rm eff}$ (independent of CPT), $|q/p| = 1$. It then follows that CP with CPT violation in mixing is defined by $z \neq 0$, and CP with T violation is through $|q/p| \neq 1$. The curves shown in Fig. 9 represent the best fit projections in Δt using Eqs (11) and (12).

The coefficients S_f and C_f are related to CP violation. Within the Weisskopf-Wigner approach, these are connected with the fundamental parameter describing indirect CP violation[46],

$$\lambda_f = \frac{q}{p}\frac{\overline{A}_f}{A_f}, \quad (14)$$

through the relations

$$S_f = 2{\rm Im}\lambda_f/(1+|\lambda_f|^2),$$
$$C_f = (1-|\lambda_f|^2)/(1+|\lambda_f|^2), \quad (15)$$

where $A_f = \langle f|\mathcal{D}|B^0\rangle$ and $\overline{A}_f = \langle f|\mathcal{D}|\overline{B}^0\rangle$ are the B^0 and $\overline{B}^0$ decay amplitudes to the final state f, with $\mathcal{D}$ the operator describing the B decay. For $f = J/\psi K_S^0$ and $f = J/\psi K_L^0$, Eq. (14) becomes

$$\lambda_f = \eta_f \frac{q}{p}\frac{\overline{A}}{A}\frac{p_K}{q_K}, \quad (16)$$

where $A = \langle J/\psi K^0|\mathcal{D}|B^0\rangle$, $\overline{A} = \langle J/\psi \overline{K}^0|\mathcal{D}|\overline{B}^0\rangle$, and $\eta_f = -1(+1)$ for $f = J/\psi K_S^0(J/\psi K_L^0)$ is associated to the CP parity of the final state. The factor p_K/q_K arises from K^0-$\overline{K}^0$ mixing, essential for the interference because B^0 and $\overline{B}^0$ decay into $J/\psi K^0$ and $J/\psi \overline{K}^0$, but not into $J/\psi \overline{K}^0$ and $J/\psi K^0$, respectively.

Assuming that the amplitude A_f can be described by a single weak phase, the two contributions to CP violation in the parameter λ_f, CP with T violation and CP with CPT violation, can be identified easily by separating it into modulus and phase, $\lambda_f = |\lambda_f|\exp(i\phi_f)$[65]. CPT invariance in the decay requires $|\overline{A}_f/A_f| = 1$[66]. For $|q/p| = 1$, experimentally well verified[51–54], it follows that $|\lambda_f| = 1$. T invariance in the time evolution followed by decay requires $\phi_f = 0$ or π, i.e. ${\rm Im}\lambda_f = 0$[67]. Instead, if A_f is the sum of two (or more) amplitudes with non-vanishing weak and strong phase differences between the two amplitudes, then we have $|\overline{A}_f/A_f| \neq 1$, even if $\mathcal{D}$ is CPT symmetric. Thus, if $|\overline{A}_f/A_f| = 1$ then we have

either both CPT symmetry in decay and a single amplitude, or an unlikely cancellation of T and CPT violation in decay amplitudes.

In the SM, B^0-$\overline{B}^0$ mixing is dominated by the box diagrams shown in Fig. 10(a), leading to $q/p \approx V_{tb}^*V_{td}/V_{tb}V_{td}^*$[19,46]. For the final state $f = J/\psi K_S^0$, the B decay is dominated by the $b \to c\bar{c}s$ tree amplitude in Fig. 10(b), followed by K^0-$\overline{K}^0$ mixing (Fig. 7). Therefore, from Eq. (16) it follows

$$\lambda_f = \eta_f \frac{V_{tb}^*V_{td}}{V_{tb}V_{td}^*}\frac{V_{cb}V_{cs}^*}{V_{cb}^*V_{cs}}\frac{V_{cs}V_{cd}^*}{V_{cs}^*V_{cd}}. \quad (17)$$

This leads to $C_f = 0$ and $S_f = {\rm Im}\lambda_f = -\eta_f \sin 2\beta$, where $\beta \equiv \arg[-(V_{cd}V_{cb}^*)/(V_{td}V_{tb}^*)]$[31] is the angle between the t and c sides of the bd unitarity triangle, illustrated in Fig. 2. In the Wolfenstein parameterization, $\beta \equiv -\arg V_{td}$. Thus, the same magnitude is expected for the CP-even and CP-odd modes up to a small correction due to CP violation in K^0-$\overline{K}^0$ oscillations. Higher-order (penguin) amplitude contributions have either the same weak phase -Fig. 7(c)- or are CKM suppressed, so that these predictions apply within the SM up to $\mathcal{O}(\lambda_c^4)$, where $\lambda_c \approx 0.226$ in the Wolfenstein parameterization[31,32]. The deviation due to the penguin contributions with different CKM phase has been estimated to be smaller than 1%[68,69]. Physics beyond the SM could modify the phase of q/p (thus S_f) and C_f, although large effects are unlikely to be generated in the latter due to the dominance of the tree amplitude in decay[70].
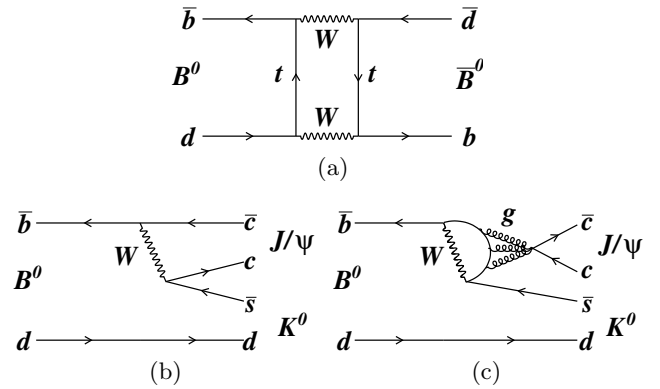

FIG. 10. (a) Box diagram corresponding to the SM short-distance contributions to B^0-$\overline{B}^0$ mixing. This contribution is matched by a diagram where the quark triplet and the W bosons are interchanged. (b) Tree and (c) penguin SM diagrams for the $B^0 \to c\bar{c}K^0$ decay. In the Wolfenstein parameterization the tree amplitude is $\mathcal{O}(\lambda_c)$, with $\lambda_c \approx 0.226$, whereas the penguin contribution is $\mathcal{O}(\lambda_c^2)$ and has the same weak phase.

IV. TIME-REVERSAL EXPERIMENT CONCEPT

We might be tempted to interpret these CP violation results as evidence for time-reversal non-invariance. The experimental study has been performed invoking $\Delta\Gamma_d = 0$ and CP invariance in mixing ($|q/p| = 1$ and $z = 0$), although the good agreement between the data points and curves observed in Fig. 9 hints that the effects of possible deviations from these assumptions are well below the statistical sensitivity of the current data. Indeed, dedicated studies have shown the good agreement of the results with and without making these assumptions[71,72]. Moreover, the results are consistent with $C_f = 0$ and $S_f \neq 0$, and therefore, according to Eq. (14), with $|\overline{A}_f/A_f| = 1$ for $|q/p| = 1$ and $\mathrm{Im}\lambda_f \neq 0$. Within the Weisskopf-Wigner approach these values are compatible with CP with CPT symmetry in decay, and CP with T violation in the interference of decay with and without mixing[65,73]. This is not, however, the question of interest here, but to set up an experiment capable to demonstrate by itself motion reversal non-invariance between states that are not CP conjugate to each other, as discussed previously.

A. Entangled neutral B mesons revisited

The solution[12–14,74,75] arises from the quantum mechanical properties imposed by the EPR entanglement[62,63] between the two neutral B mesons produced in the $\Upsilon(4S)$ resonance decay. Just as one B meson in the entangled pair is prepared in the $\overline{B}^0$ or B^0 states at the time when the other B is observed as a B^0 or $\overline{B}^0$ by a decay into $\ell^+ X$ or $\ell^- \overline{X}$, respectively, the first decay of one B into the final states $J/\psi K_S^0$ or $J/\psi K_L^0$ prepares the other B into well defined, orthogonal linear combinations of B^0 and $\overline{B}^0$ states. In fact, this idea offers the opportunity to explore separately time reversal, CP and CPT symmetries, selecting appropriately different transitions defined by different decay channels.

For the entangled state of the two mesons produced by the $\Upsilon(4S)$ decay, the individual state of each neutral B meson is not defined before its collapse as a filter imposed by the observation of the decay. Thus, the state $|\Upsilon\rangle$ in Eq. (8) can be written in terms of any pair of orthogonal states of the individual B mesons, i.e. a linear combination of B^0 and $\overline{B}^0$, that we denote B_+, and its orthogonal state, B_-,

$$|\Upsilon\rangle = \frac{1}{\sqrt{2}}\left[|B_+(t_1)\rangle|B_-(t_2)\rangle - |B_-(t_1)\rangle|B_+(t_2)\rangle\right]. \quad (18)$$

As in Eq. (8), the time evolution (including mixing) preserves only $|B_+\rangle|B_-\rangle$ and $|B_-\rangle|B_+\rangle$ terms.

Neglecting CP violation in K^0-$\overline{K}^0$ mixing, which holds within $\mathcal{O}(10^{-3})$[31], and assuming that $B^0 \to J/\psi K^0$ and

$\overline{B}^0 \to J/\psi \overline{K}^0$, the normalized states

$$|B_+\rangle = \mathcal{N}\left(|B^0\rangle + \frac{A}{\overline{A}}|\overline{B}^0\rangle\right),$$

$$|B_-\rangle = \mathcal{N}\left(|B^0\rangle - \frac{A}{\overline{A}}|\overline{B}^0\rangle\right), \quad (19)$$

where $\mathcal{N} = |\overline{A}|/\sqrt{|A|^2 + |\overline{A}|^2}$, have the property that the former decays into $J/\psi K_L^0$, but not into $J/\psi K_S^0$, and the latter into $J/\psi K_S^0$, but not into $J/\psi K_L^0$[61,75].

The proof is as follows. Adopting the same sign convention as in Eq. (13)[76], and assuming CPT invariance in kaon mixing, we have

$$|K_S^0\rangle = \mathcal{N}_K\left(p_K|K^0\rangle - q_K|\overline{K}^0\rangle\right),$$

$$|K_L^0\rangle = \mathcal{N}_K\left(p_K|K^0\rangle + q_K|\overline{K}^0\rangle\right), \quad (20)$$

with $\mathcal{N}_K = 1/\sqrt{|p_K|^2 + |q_K|^2}$. In the absence of wrong-strangeness B decays, $\langle J/\psi \overline{K}^0|\mathcal{D}|B^0\rangle = \langle J/\psi K^0|\mathcal{D}|\overline{B}^0\rangle = 0$, it is straightforward to show that

$$\langle J/\psi K_S^0(K_L^0)|\mathcal{D}|B_+\rangle = \mathcal{N}\mathcal{N}_K\left[p_K A - (+)q_K A\right],$$

$$\langle J/\psi K_L^0(K_S^0)|\mathcal{D}|B_-\rangle = \mathcal{N}\mathcal{N}_K\left[p_K A - (+)q_K A\right]. \quad (21)$$

Assuming now CP invariance in K^0-$\overline{K}^0$ mixing, we have $p_K = q_K$ and the above expressions yield

$$\langle J/\psi K_L^0|\mathcal{D}|B_+\rangle = \langle J/\psi K_S^0|\mathcal{D}|B_-\rangle = 2p_K\mathcal{N}\mathcal{N}_K A,$$

$$\langle J/\psi K_S^0|\mathcal{D}|B_+\rangle = \langle J/\psi K_L^0|\mathcal{D}|B_-\rangle = 0, \quad (22)$$

hence B_+ cannot decay into $J/\psi K_S^0$ and B_- cannot into $J/\psi K_L^0$. Note that using Eq. (14) and inverting Eq. (20) it is straightforward to obtain Eq. (16) and the relation $\lambda_{J/\psi K_L^0} = -\lambda_{J/\psi K_S^0}$, as introduced in Sec. III B. The fact that the two amplitude ratios differ only by a minus sign is of key importance for the definition of the $B_\pm$ states. According to the definition in Eq. (19), these states are well behaved under B^0 and $\overline{B}^0$ rephasing, although they are not CP eigenstates independent of the flavor of the decay channel due to arbitrary quark phases and possible deviations from $|A/\overline{A}| = 1$.

The observation of the decay to the $J/\psi K_S^0$ ($J/\psi K_L^0$) final state at time t_1 generates an automatic transfer of information to the (still living) partner meson. Hence, the other B meson at that time is in a B_+ (B_-) state because this is the state that cannot decay into $J/\psi K_S^0$ ($J/\psi K_L^0$). We call the quantum preparation of the initial state at t_1, using the filter imposed by the observation at t_1, a "B_+ (B_-) tag". Sometimes it is referred to as a "CP tag"[77] because it is defined through decays into CP-eigenstate final states. The B_+ or B_- states prepared by entanglement at t_1 evolve in time until they are observed at some later time t_2 in a decaying final state filtering another linear combination state. For convenience, we restrict to flavor-specific final states $\ell^- \overline{X}$ and $\ell^+ X$ that can be used to filter, assuming no wrong-sign B decays, the state of the B meson at t_2 as $\overline{B}^0$ and B^0, respectively.

Initial states B^0 and $\overline{B}^0$ can be prepared similarly, as already discussed in Sec. III A. The observation of the

decay to $\ell^- \overline{X}$ ($\ell^+ X$) at time t_1 dictates that the other B meson at that time is in a B^0 ($\overline{B}^0$) state because this state cannot decay into $\ell^- \overline{X}$ ($\ell^+ X$). As before, this requires assuming the absence of wrong-sign B decays, i.e. $B^0 \to \ell^- \overline{X}$ and $\overline{B}^0 \to \ell^+ X$ do not occur. We refer to the quantum preparation of this initial state at t_1 as "B^0 ($\overline{B}^0$) tag". The B^0 or $\overline{B}^0$ states prepared by entanglement at t_1 evolve in time until they are observed at some later time t_2 in a decaying final state filtering a given B^0 and $\overline{B}^0$ linear combination state, which we select B_+ or B_- by observing the appropriate decay channels.

By virtue of the EPR correlation of Eq. (18), B_+ and B_- have been defined as states orthogonal to the states, denoted as $B_-^\perp$ and $B_+^\perp$, defined through the filter imposed by the observation at t_1 of the decay into $J/\psi K_S^0$ and $J/\psi K_L^0$, respectively, i.e. $\langle B_+ | B_-^\perp \rangle = \langle B_- | B_+^\perp \rangle = 0$. The exchange of initial and final states with identical boundary conditions required by motion reversal imposes that the basis of tagging states (B_+, B_-) must be identical to the basis of states filtered by decay $(B_+^\perp, B_-^\perp)$. This condition is met when B_+ and B_- (and thus $B_+^\perp$ and $B_-^\perp$) are orthogonal to each other. It is then straightforward to prove that $\langle B_- | B_+ \rangle = 0$ if $|A/\overline{A}| = 1$. For this to hold, the decay amplitude A should have only one weak phase, as it is expected to apply at 1% level or better for $B^0 \to J/\psi K^0$ and $\overline{B}^0 \to J/\psi \overline{K}^0$, and have CPT symmetry in the decay amplitude (see Sec. III B).

To clarify the foundations of the time-reversal experiment, consider the case illustrated in Fig. 11. In the top panel, the first B decays into a $\ell^+ X$ final state (for example a semileptonic final state producing a positively-charged prompt lepton or an hadronic final state with a positively-charged kaon). This final state filters the quantum-mechanical state of the other B at time t_1 as $\overline{B}^0$. The surviving meson tagged as $\overline{B}^0$ is observed later at t_2 to decay into a final state $J/\psi K_L^0$ that filters the B meson to be in a B_+ state. Therefore, the event class $(\ell^+ X, J/\psi K_L^0)$, encapsulating a time ordering, undergoes a transition $\overline{B}^0 \to B_+$ in the elapsed time $t = t_2 - t_1$. This transition has, according to the convention in Eq. (9), a decay time difference $\Delta t = t > 0$. As shown in the bottom panel, T transformation demands to set up the conditions for the mirrored transition $B_+ \to \overline{B}^0$. The B_+ tag requires the first B to decay into the $J/\psi K_S^0$ final state, whereas the surviving meson tagged at t_1 as B_+ has to be observed at t_2 through its decay into a $\ell^- \overline{X}$ flavor specific final state. The time-ordered event class is now $(J/\psi K_S^0, \ell^- \overline{X})$, which according to Eq. (9) yields a decay time difference $\Delta t < 0$. Thus and from now on, "$\Delta t > 0$" ("$\Delta t < 0$") will refer to the time ordering in an event class with a flavor- (CP-) eigenstate decay channel appearing first. Note that this non-trivial T transformation is not defined by the "Δt reversal" obtained just by flipping the time ordering of the decay channels for a given event class. For this to be achieved, EPR entanglement together with the availability of both flavor- and CP-eigenstate decay modes to filter appropriate neutral B states, has been key for the quantum preparation of

the B-meson initial state in the transition and its motion-reversed version; the problem of particle instability has been thus avoided.

B. Transitions among B meson states

For the four initial states B^0, $\overline{B}^0$, B_+, and B_- prepared by entanglement, and the four final states B^0, $\overline{B}^0$, B_+, and B_- available through decay, it is possible to construct eight transitions and their corresponding time-ordered event classes (f_1, f_2) given in Table I[75]. In this notation, the final state f_1 is observed at time t_1 and the final state f_2 is observed at time $t_2 = t_1 + t$, where $t > 0$ is the elapsed time. The matching between event classes and transitions applies under the assumption of absence of wrong-strangeness and wrong-sign B decays, CP invariance in K^0-$\overline{K}^0$ mixing, and $|\overline{A}/A| = 1$. Recently an extended discussion, including wrong-strangeness and wrong-sign B decays, has been presented[78].

The observation of an asymmetry between the probabilities for transitions on the right and left panels of Table I,

$$|\langle \overline{B}^0 | \mathcal{U}(t) | B_- \rangle|^2 - |\langle B_- | \mathcal{U}(t) | \overline{B}^0 \rangle|^2,$$
$$|\langle B_- | \mathcal{U}(t) | B^0 \rangle|^2 - |\langle B^0 | \mathcal{U}(t) | B_- \rangle|^2,$$
$$|\langle \overline{B}^0 | \mathcal{U}(t) | B_+ \rangle|^2 - |\langle B_+ | \mathcal{U}(t) | \overline{B}^0 \rangle|^2,$$
$$|\langle B_+ | \mathcal{U}(t) | B^0 \rangle|^2 - |\langle B^0 | \mathcal{U}(t) | B_+ \rangle|^2, \quad (23)$$

will be an unambiguous demonstration of motion reversal in time evolution of states that are not CP conjugate to each other. Here, $\mathcal{U}(t)$ is the time-evolution operator determined by the effective Hamiltonian $\mathcal{H}_{\text{eff}}$. Note that the notation has been changed in comparison to Sec. II A since t denotes now the elapsed time. We immediately realize that each of the four independent time-reversal comparisons in Table I uses a pair of time-ordered event classes involving four different final states at different times, $\ell^+ X$ and $\ell^- \overline{X}$ at times t_1 (or t_2) and t_2 (or t_1), and $J/\psi K_S^0$ and $J/\psi K_L^0$ at times t_2 (or t_1) and t_1 (or t_2), respectively. Therefore, time-reversal tests require the comparison of probabilities for event classes with opposite time ordering (opposite Δt sign) and different observed flavor- and CP-eigenstate final states, as illustrated in Fig. 12[75].

With the same approximations, differences like

$$|\langle B^0 | \mathcal{U}(t) | B_- \rangle|^2 - |\langle B_- | \mathcal{U}(t) | \overline{B}^0 \rangle|^2, \quad (24)$$

or

$$|\langle B_- | \mathcal{U}(t) | B^0 \rangle|^2 - |\langle B_- | \mathcal{U}(t) | \overline{B}^0 \rangle|^2, \quad (25)$$

probe CPT and CP symmetry, respectively, in the time evolution of B^0-$\overline{B}^0$ transitions. For each of these cases there are also four independent asymmetries, although clearly not all comparisons involving time reversal, CP, and CPT transformations are independent. Whereas CP transformation requires the comparison of pairs of time-ordered event classes with different flavor-specific final
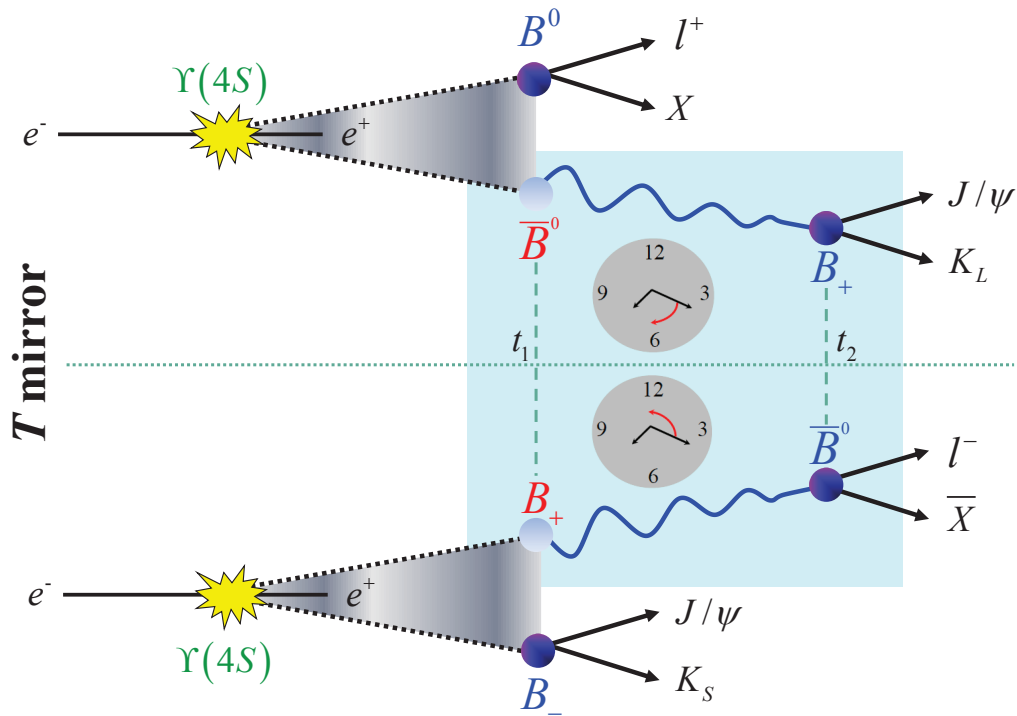
FIG. 11. Basic concept of the time-reversal experiment. Electron-positron collisions at the asymmetric B factory produce $\Upsilon(4S)$ resonances, which decay via strong interaction to an entangled pair of B mesons. When one B meson decays at t_1, the identity of the other is "tagged" without measuring it specifically. In the top panel, the B meson observed to decay to the final state $\ell^+ X$ at t_1 transfers information to the other meson and dictates that it is in a $\overline{B}^0$ state. This surviving meson tagged as $\overline{B}^0$ is observed at t_2 to decay into a final state $J/\psi K_L^0$ that filters the B meson to be in a B_+ state, a linear combination of B^0 and $\overline{B}^0$ states. This case corresponds to a transition $\overline{B}^0 \to B_+$. To study time reversal we have to compare the rate at which this transition occurs to the rate of the time-reversed transition, $B_+ \to \overline{B}^0$ (bottom panel).

states, but common CP-eigenstate final state and same Δt sign, CPT demands a common flavor-specific final state, different CP-eigenstate final states, and opposite Δt sign (see Fig. 12)[75]. Therefore, the time-reversal case is the most challenging.

V.   BABAR TIME-REVERSAL ANALYSIS

The BABAR detector recorded an integrated luminosity of 518 fb^{-1} of data, of which 424 fb^{-1} were taken at a c.m. energy corresponding to the mass of the $\Upsilon(4S)$ resonance, 28 and 13.6 fb^{-1} around the $\Upsilon(3S)$ and $\Upsilon(2S)$ resonances (10.36 and 10.02 GeV), 4 fb^{-1} above the $\Upsilon(4S)$, and 48 fb^{-1} below the resonances [44 fb^{-1} at a c.m. energy 40 MeV below the $\Upsilon(4S)$][58]. These luminosities correspond to about 470×10^6 $B\overline{B}$, 690×10^6 $c\overline{c}$, and 500×10^6 $\tau^+\tau^-$ pairs, and 121×10^6 $\Upsilon(3S)$ and 99×10^6 $\Upsilon(2S)$ resonances. For the time-reversal analysis[1] BABAR used all $B\overline{B}$ and $\Upsilon(4S)$ off-resonance data.

The BABAR detector, sketched in Fig. 13, was designed as a general purpose detector for e^+e^- annihilation physics[59]. Surrounding the interaction point is a five-layer, double-sided Silicon Vertex Tracker (SVT), which measures the angles and impact parameters of charged particle tracks. A 40-layer Drift Chamber (DC) surrounds the SVT and provides measurements of the momenta for charged particles. Charged hadron identification is achieved through measurements of energy-loss in the tracking system and the Cherenkov angle obtained from a Detector of Internally Reflected Cherenkov light (DIRC). A CsI(Tl) electromagnetic calorimeter (EMC) provides photon detection, electron identification, and π^0 reconstruction. These components are inserted inside a solenoid magnet, which provides a 1.5 T magnetic field. The flux return of the magnet (IFR) is instrumented with resistive plate chambers and limited streamer tubes in order to detect muons and K_L^0s[58]. Figure 14 illustrates the transverse view of the computer reconstruction of a $B\overline{B}$ event. The detector performance has been very sta-
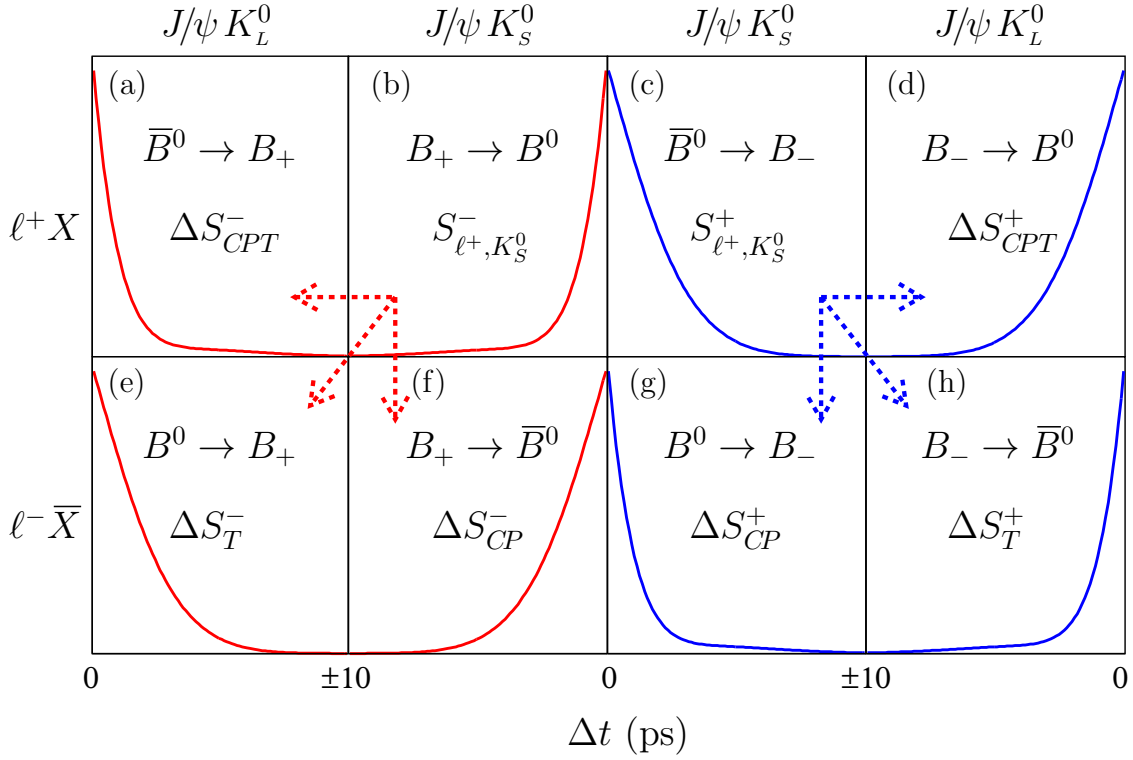
FIG. 12. Expected time-dependent probability distributions for the eight time-ordered event classes given in Table I, shown as a planar map. They are identified by the flavor-specific ($\ell^- \overline{X}$, $\ell^+ X$) and CP-eigenstate ($J/\psi K_S^0$, $J/\psi K_L^0$) decay products and the time ordering. The dashed arrows in the left (red) and right (blue) panels indicate the time-ordered event classes connected by the three symmetries, CP (vertical), T (oblique), and CPT (horizontal), independently of each other. The two panels (red, blue) of t-reverse decay channels are unconnected by the symmetries.

TABLE I. Time-ordered event classes (f_1, f_2) and their corresponding transitions between B meson states. The matching between event classes and transitions applies under the assumption of absence of wrong-strangeness and wrong-sign B decays, a single weak amplitude, i.e. $|\overline{A}/A| = 1$, and no CP violation in K^0-$\overline{K}^0$ mixing. The event classes and transitions on the right panel (Time reversed) are the time-reversed versions of those in the left panel (Reference).

Reference		Time reversed	
Event class	Transition	Event class	Transition
$(\ell^+ X, J/\psi K_L^0)$	$\overline{B}^0 \to B_+$	$(J/\psi K_S^0, \ell^- \overline{X})$	$B_+ \to \overline{B}^0$
$(J/\psi K_S^0, \ell^+ X)$	$B_+ \to B^0$	$(\ell^- \overline{X}, J/\psi K_L^0)$	$B^0 \to B_+$
$(\ell^+ X, J/\psi K_S^0)$	$\overline{B}^0 \to B_-$	$(J/\psi K_L^0, \ell^- \overline{X})$	$B_- \to \overline{B}^0$
$(J/\psi K_L^0, \ell^+ X)$	$B_- \to B^0$	$(\ell^- \overline{X}, J/\psi K_S^0)$	$B^0 \to B_-$

ble over the nine years of operation, supporting a broad flavor physics program.

Although the CP-violation and time-reversal analysis concepts are fundamentally different, the experimental analyses are closely connected to each other. Reconstruction algorithms, event selection criteria, calibration techniques and descriptions of the background composition are common[64]. However, the selected signal events for the time-reversal measurement require somewhat different treatment.

A. Event reconstruction and selection

In addition to $J/\psi K_S^0$, $\psi(2S)K_S^0$ and $\chi_{c1}K_S^0$ decay modes are also considered; all these three final states have CP-odd parity and are hereafter denoted generically as $c\bar{c}K_S^0$. The $c\bar{c}$ particle states are reconstructed in the decay channels $J/\psi, \psi(2S) \to e^+ e^-, \mu^+ \mu^-$, $\psi(2S) \to J/\psi \pi^+ \pi^-$, and $\chi_{c1} \to J/\psi \gamma$. Whereas K_S^0 mesons decay near the collision point and are reconstructed through their decays into $\pi^+ \pi^-$ and $\pi^0 \pi^0$ (the latter only for $J/\psi K_S^0$), the long-living K_L^0 mesons pass through the tracking systems undetected and are reconstructed by their hadronic interactions in the EMC and/or the IFR and the J/ψ in the B decay. The background rejection relies on vetoes to specific B decay modes, and on an-
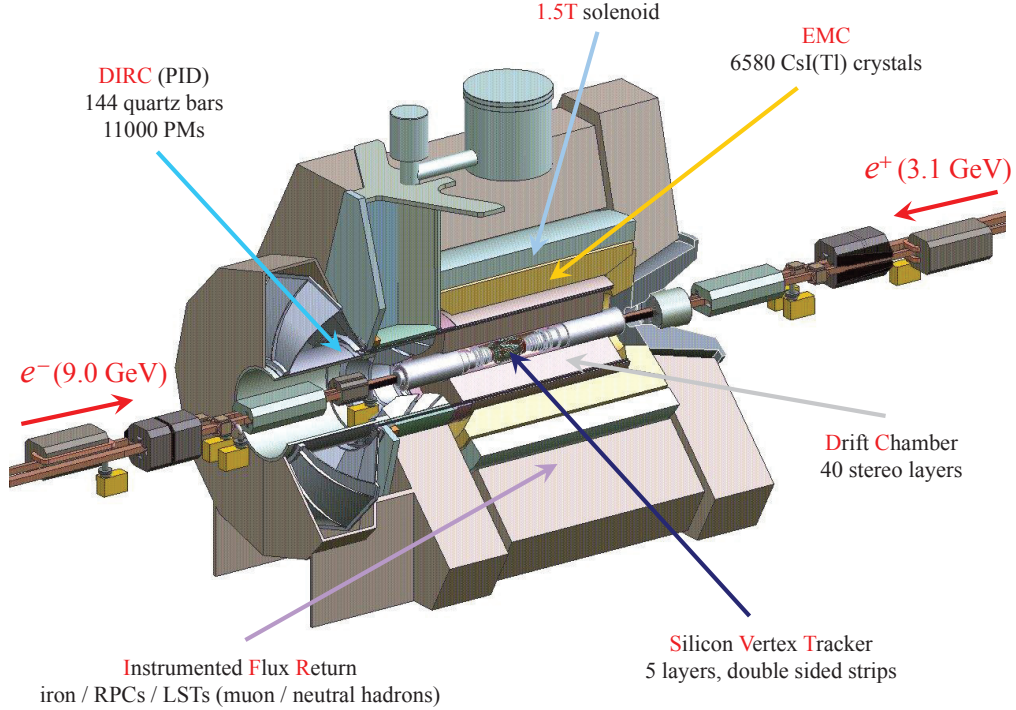
FIG. 13. A sketch of the *BABAR* detector. The five subsystems and the solenoid magnet providing the 1.5 T magnetic field are indicated. Source: *BABAR* Collaboration.

gular and event shape variables to suppress continuum events arising from $e^+e^- \rightarrow q\bar{q}$, $q = u, d, s$ reactions. These variables exploit the different topology of $q\bar{q}$ and $B\bar{B}$ events, jet-like for the former and spherical for the latter, consequence of the large mass difference between light and b quarks.

B meson candidates decaying to $J/\psi K_L^0$ are characterized by the energy difference $\Delta E = E_B^* - E_{\text{beam}}^*$ between the B energy and the beam energy in the e^+e^- c.m. frame, while for the $c\bar{c}K_S^0$ final states the beam-energy substituted mass, $m_{\text{ES}} = \sqrt{(E_{\text{beam}}^*)^2 - |\mathbf{p}_B^*|^2}$, is used, where $\mathbf{p}_B^*$ is the B momentum in the c.m. frame. These two kinematic variables are based on the fact that B mesons are produced almost at rest in c.m. frame and the beam energies are precisely known. Figure 15 shows the m_{ES} and ΔE data distributions for the final sample of about 7800 $c\bar{c}K_S^0$ signal events with purities ranging from 87 to 96%, and 5800 $J/\psi K_L^0$ signal events with purities around 60%.

Since the mass of the $\Upsilon(4S)$ is only slightly higher than twice the mass of the B meson, no additional particles are produced. Thus, the flavor identity of the B meson not associated with the reconstructed $c\bar{c}K_S^0$ or $J/\psi K_L^0$ final state is determined from the remaining particles in the event, on the basis of the charges of prompt leptons and kaons, pions from $D^{*+} \rightarrow D^0\pi^+$ decays, and high-momentum charged particles. The notation $\ell^- \overline{X}$ ($\ell^+ X$) introduced previously denotes all these inclusive

final states that identify the flavor of the B as $\overline{B}^0$ (B^0). In practice, these flavor identity signatures are combined using a neural network whose output is used to divide the events into six hierarchical, mutually exclusive flavor categories of increasing misidentification probability. The proper time difference between the decay of the two B mesons, Δt, is measured by the separation of the two decay vertices along the e^+e^- collision axis and the known boost, as discussed in Sec. III.

Besides the CP eigenstate final states, other high-statistics, flavor-specific final states like $B^0 \rightarrow D^{*-}\pi^+$ and $B^0 \rightarrow J/\psi K^{*0}[\rightarrow K^+\pi^-]$ (and their CP conjugates) are reconstructed, and are used for calibrating the Δt resolution and the flavor misidentification probability. Charged B meson decays like $B^{\pm} \rightarrow J/\psi K^{\pm}, \psi(2S)K^{\pm}, J/\psi K^{*\pm}$ are likewise detected and used for systematic checks.

B. Signal data treatment and results

Assuming $\Delta\Gamma_d = 0$, the time dependence of each of the eight transitions depicted in Fig. 12 can be parameterized in a model-independent way as

$$\frac{g_{\alpha,\beta}^{\pm}(t)}{e^{-\Gamma_d t}} \propto 1 + S_{\alpha,\beta}^{\pm} \sin(\Delta m_d t) + C_{\alpha,\beta}^{\pm} \cos(\Delta m_d t), \quad (26)$$
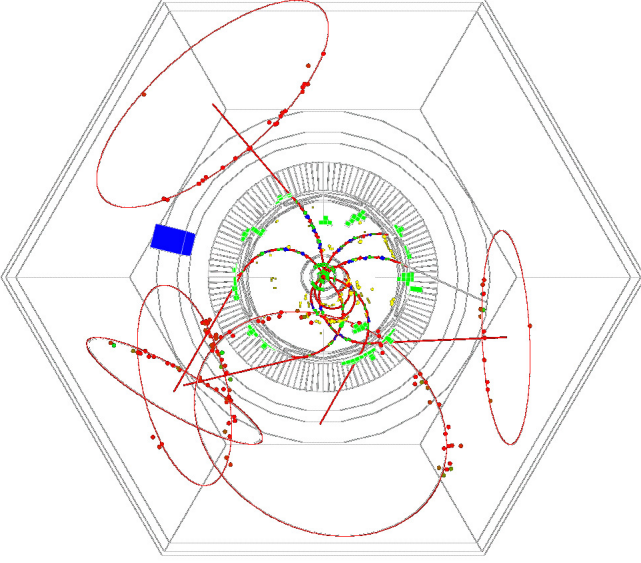
FIG. 14. Transverse view of the computer reconstruction of a $B\bar{B}$ event in the BABAR detector. The display shows the decay products of the two B mesons as curved tracks (in red) in the central region of the detector (SVT and DC). Some particles deposit energy in the EMC calorimeter (green and blue blocks). Particle identification is assisted by measuring the Cherenkov rings (DIRC). Source: BABAR Collaboration.
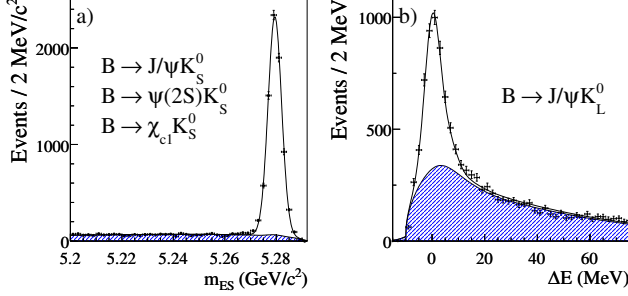

FIG. 15. (a) m_{ES} and (b) ΔE distributions for the final sample of neutral B decays reconstructed in the $c\bar{c}K_S^0$ and $J/\psi K_L^0$ final states, respectively. The shaded regions represent the estimated background contributions.

where the lower indices $\alpha = \ell^+, \ell^-$ and $\beta = K_S^0, K_L^0$ stand for the final reconstructed decay modes $\ell^+ X$, $\ell^- \bar{X}$ and $c\bar{c}K_S^0$, $J/\psi K_L^0$, respectively, and the upper indices encapsulate the time ordering, $(+)$ for B^0 or $\bar{B}^0$ tagged states and $(-)$ for B_+ or B_- tagged states. This expression is analogous to Eq. (11) with the distinction that is associated to eight pairs $(S_{\alpha,\beta}^\pm, C_{\alpha,\beta}^\pm)$ instead of only one, and $t > 0$.

The pairs of parameters $(S_{\alpha,\beta}^\pm, C_{\alpha,\beta}^\pm)$ are determined by a maximum likelihood fit to the measured Δt distributions of the four signal samples in which one B meson

is reconstructed in a $c\bar{c}K_S^0$ or $J/\psi K_L^0$ decay mode, and the flavor content of the other B is identified through a $\ell^- \bar{X}$ or $\ell^+ X$ decay mode. Neglecting time resolution, the elapsed time between the first and second decay is $t = \Delta t$ for flavor tags, and $t = -\Delta t$ for $B_\pm$ tags. As illustrated in Fig. 16, time resolution mixes events with positive and negative true Δt, i.e. a true event class $(\ell^+ X, J/\psi K_L^0)$, corresponding to a $\bar{B}^0 \to B_+$ transition, might appear reconstructed as $(J/\psi K_L^0, \ell^+ X)$, corresponding to a $B_- \to B^0$ transition, and vice versa. To determine separately the coefficients for event classes with true positive Δt (flavor tag) or true negative Δt ($B_\pm$ tag), it is necessary to unfold the time ordering and the Δt resolution. This is accomplished by using a signal probability-density-function for the four distributions of the form

$$\mathcal{H}_{\alpha,\beta}(\Delta t) = g_{\alpha,\beta}^+(\Delta t_{\text{true}})H(\Delta t_{\text{true}}) \otimes \mathcal{R}(\delta t; \sigma_{\Delta t}) +$$
$$g_{\alpha,\beta}^-(-\Delta t_{\text{true}})H(-\Delta t_{\text{true}}) \otimes \mathcal{R}(\delta t; \sigma_{\Delta t}), \tag{27}$$

where Δt_{true} is the signed difference of proper times between the two B decays in the limit of perfect Δt resolution, H is the Heaviside step function, $\mathcal{R}(\delta t; \sigma_{\Delta t})$ is the resolution function, with $\delta t = \Delta t - \Delta t_{\text{true}}$, and $\sigma_{\Delta t}$ is the estimate of the Δt uncertainty obtained by the reconstruction algorithms. This unfolding procedure, which requires good Δt resolution and excellent knowledge of the resolution function, especially in the low $|\Delta t|$ region, is of critical importance to resolve the time ordering and represents in practice the main experimental challenge of this time-reversal analysis[1] in comparison to the associated CP violation analysis[64].

From the eight pairs of signal coefficients, reported in the left panel of Table II, one might construct two sets $(\pm)$ of three pairs each of independent asymmetry parameters, $(\Delta S_T^\pm, \Delta C_T^\pm)$, $(\Delta S_{CP}^\pm, \Delta C_{CP}^\pm)$, and $(\Delta S_{CPT}^\pm, \Delta C_{CPT}^\pm)$, as illustrated in Fig. 12 and also shown in the right panel of Table II. There are multiple choices to define the asymmetry parameters but for convenience two sets (panels in the first and second columns, and in the third and fourth columns of Fig. 12) of asymmetries related to each of the three discrete symmetries are chosen. The reference transitions are taken by convention $B_+ \to B^0$ and $\bar{B}^0 \to B_-$, corresponding to event classes $(c\bar{c}K_S^0, \ell^+ X)$ and $(\ell^+ X, c\bar{c}K_S^0)$, respectively (see Fig. 12 and Table II). This choice has the advantage that the breaking of time-reversal symmetry would directly manifest itself through any nonzero value of $\Delta S_T^\pm$ or any difference between $\Delta S_{CP}^\pm$ and $\Delta S_{CPT}^\pm$.

Systematic uncertainties in the measurement of the coefficients and asymmetry parameters in Table II are dominated by the knowledge of the Δt resolution and background composition of event classes containing $J/\psi K_L^0$ final states, and any possible deviation of the experimental procedure observed in detailed Monte Carlo simulations[58]. Besides, the experiment has performed a number of cross-checks, based on both simulated and data
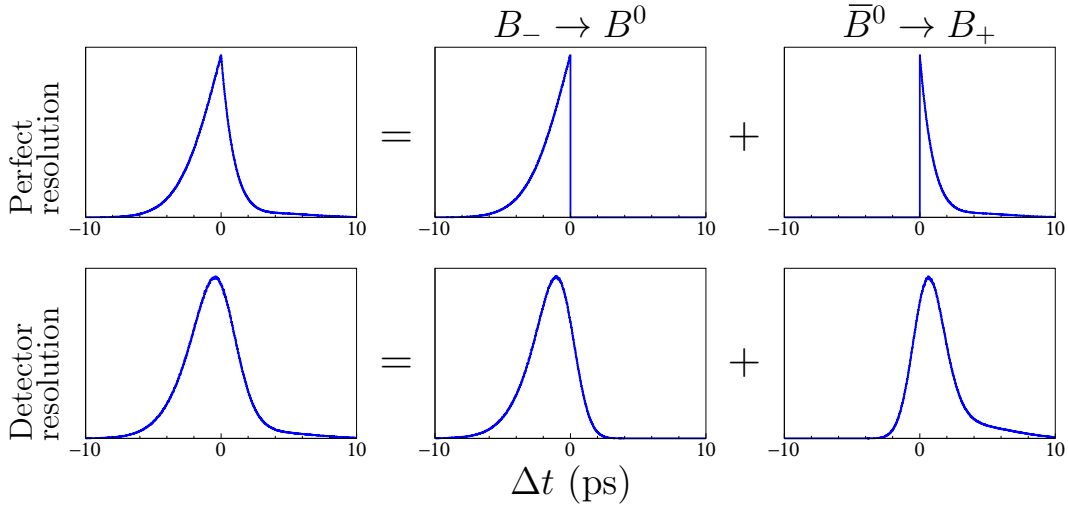
$$B_- \to B^0 \qquad \overline{B}^0 \to B_+$$

FIG. 16. Unfolding of the measured Δt distributions: the reconstructed Δt distribution (bottom left) is unfolded to disentangle the Δt resolution function and the true Δt distribution (top left) used to define the $B_\pm$ (true $\Delta t < 0$, top middle) and flavor (true $\Delta t > 0$, top right) tags. The Δt resolution mixes true $B_\pm$ or flavor tags with fake flavor or $B_\pm$ tags (bottom middle and bottom right), respectively. The case shown here corresponds to a signal sample in which the two B mesons have been reconstructed in the decay modes $J/\psi K_L^0$ and $\ell^+ X$. The event classes are $(J/\psi K_L^0, \ell^+ X)$ and $(\ell^+ X, J/\psi K_L^0)$, corresponding to transitions $B_- \to B^0$ and $\overline{B}^0 \to B_+$, respectively.

control samples, to assess the robustness of the results. Of special relevance is the check performed using event classes where the neutral B meson reconstructed in the $c\bar{c}K_S^0$ or $J/\psi K_L^0$ final states is replaced by a charged B decaying to $c\bar{c}K^\pm$ and $J/\psi K^{*+}$, respectively. It is found that all coefficients and parameters, shown in Table II, are consistent with zero.

C. Interpretation of results and significance

The ability of this analysis to describe the data can be assessed by visualizing the rate differences between the transitions and their time-reversed conjugates in Table I. The inequalities among probabilities are better determined in the form of asymmetries along the lines of Eq. (10). For transition $\overline{B}^0 \to B_-$ (first entry in Table I),

$$A_T(\Delta t) = \frac{\mathcal{H}_{\ell^-, K_L^0}^-(\Delta t) - \mathcal{H}_{\ell^+, K_S^0}^+(\Delta t)}{\mathcal{H}_{\ell^-, K_L^0}^-(\Delta t) + \mathcal{H}_{\ell^+, K_S^0}^+(\Delta t)}, \quad (28)$$

where $\mathcal{H}_{\alpha, \beta}^\pm(\Delta t) = \mathcal{H}_{\alpha, \beta}(\pm \Delta t) H(\Delta t)$. With this construction, $A_T(\Delta t)$ is defined only for positive Δt values. Neglecting reconstruction effects,

$$A_T(t) \approx \frac{\Delta S_T^+}{2} \sin(\Delta m_d t) + \frac{\Delta C_T^+}{2} \cos(\Delta m_d t). \quad (29)$$

The three other asymmetries, corresponding to the last three entries in Table I, are constructed analogously and have the same time dependence, with ΔS_T^+ replaced by ΔS_T^-, $\Delta S_{CP}^- - \Delta S_{CPT}^-$, and $\Delta S_{CP}^+ - \Delta S_{CPT}^+$, respectively, and equally for ΔC_T^+.

Figure 17 shows the four time-reversal asymmetries constructed in this way. The data are well described by the red solid curves, which represent the projection of the best fit to the eight $(S_{\alpha,\beta}^\pm, C_{\alpha,\beta}^\pm)$ pairs, as reported in Table II. These curves deviate significantly from the dashed blue curves, which represent the fit projection for time-reversal invariance, i.e. $\Delta S_T^\pm = 0$, $\Delta C_T^\pm = 0$, $\Delta S_{CP}^\pm = \Delta S_{CPT}^\pm$, and $\Delta C_{CP}^\pm = \Delta C_{CPT}^\pm$. The fact that the dashed blue curves are not identically zero is a consequence of experimental effects, in particular the asymmetry with respect to $\delta t = 0$ of the time resolution function.

All eight $C_{\alpha,\beta}^\pm$ in Table II are compatible with zero, therefore the $|\overline{A}/A| = 1$ condition discussed in Sec. IV A is validated within errors and the association between event classes and transitions in Table I is confirmed. It follows that the observation $\Delta S_T^\pm \neq 0$ and $\Delta S_{CP}^\pm \neq \Delta S_{CPT}^\pm$ in Table II is an unambiguous, direct detection of time-reversal violation in the time evolution of neutral B mesons, obtained through motion reversal in transitions that are not CP conjugate to each other. The violation of time-reversal symmetry is also clearly seen through the large differences between the red solid and dashed blue curves in all four asymmetries shown in Fig. 17.

The significance of the observed time-reversal violation is evaluated on the basis of changes in log-likelihood value $\ln \mathcal{L}$ with respect to the maximum $(-2\Delta \ln \mathcal{L})$. The difference $-2\Delta \ln \mathcal{L}$ between the fit without T violation and the best fit is 226, including systematic uncertainties. Assuming Gaussian statistics, this corresponds to a significance of 14σ, evaluated from the upper integral at $-2\Delta \ln \mathcal{L}$ of the χ^2 probability distribution for 8 degrees of freedom[79] (p-value)[31]. Figure 18 shows p-value

TABLE II. Measured values of the $S^{\pm}_{\alpha,\beta}$ and $C^{\pm}_{\alpha,\beta}$ coefficients, and of the asymmetry parameters, defined as differences among coefficients for symmetry-transformed transitions as depicted in Fig. 12[1]. The first uncertainty is statistical and the second systematic. The lower indices ℓ^-, ℓ^+, K^0_S, and K^0_L stand for reconstructed decay modes that identify the B meson state as $\overline{B}^0$, B^0 and B_-, B_+, respectively, and the upper indices encapsulate the time ordering, $(+)$ when the decay to ℓ^- and ℓ^+ occurs first and $(-)$ otherwise. The asymmetry parameters $\Delta S^{\pm}_T$, $\Delta C^{\pm}_T$ and the differences $\Delta S^{\pm}_{CP} - \Delta S^{\pm}_{CPT}$, $\Delta C^{\pm}_{CP} - \Delta C^{\pm}_{CPT}$ are all motion-reversal violating. The first column refers to the index labelling in Fig. 12.

Transition	Coefficient	Result	Asymmetry parameter	Result
(b) $B_+ \to B^0$	$S^-_{\ell^+,K^0_S}$	$-0.66 \pm 0.06 \pm 0.04$	Reference	
	$C^-_{\ell^+,K^0_S}$	$-0.05 \pm 0.06 \pm 0.03$	Reference	
(e) $B^0 \to B_+$	$S^+_{\ell^-,K^0_L}$	$0.51 \pm 0.17 \pm 0.11$	ΔS^-_T	$1.17 \pm 0.18 \pm 0.11$
	$C^+_{\ell^-,K^0_L}$	$-0.01 \pm 0.13 \pm 0.08$	ΔC^-_T	$0.04 \pm 0.14 \pm 0.08$
(a) $\overline{B}^0 \to B_+$	$S^+_{\ell^+,K^0_L}$	$-0.69 \pm 0.11 \pm 0.04$	ΔS^-_{CPT}	$-0.03 \pm 0.13 \pm 0.06$
	$C^+_{\ell^+,K^0_L}$	$-0.02 \pm 0.11 \pm 0.08$	ΔC^-_{CPT}	$0.03 \pm 0.12 \pm 0.08$
(f) $B_+ \to \overline{B}^0$	$S^-_{\ell^-,K^0_S}$	$0.67 \pm 0.10 \pm 0.08$	ΔS^-_{CP}	$1.33 \pm 0.12 \pm 0.06$
	$C^-_{\ell^-,K^0_S}$	$0.03 \pm 0.07 \pm 0.04$	ΔC^-_{CP}	$0.08 \pm 0.10 \pm 0.04$
(c) $\overline{B}^0 \to B_-$	$S^+_{\ell^+,K^0_S}$	$0.55 \pm 0.09 \pm 0.06$	Reference	
	$C^+_{\ell^+,K^0_S}$	$0.01 \pm 0.07 \pm 0.05$	Reference	
(h) $B_- \to \overline{B}^0$	$S^-_{\ell^-,K^0_L}$	$-0.83 \pm 0.11 \pm 0.06$	ΔS^+_T	$-1.37 \pm 0.14 \pm 0.06$
	$C^-_{\ell^-,K^0_L}$	$0.11 \pm 0.12 \pm 0.08$	ΔC^+_T	$0.10 \pm 0.14 \pm 0.08$
(d) $B_- \to B^0$	$S^-_{\ell^+,K^0_L}$	$0.70 \pm 0.19 \pm 0.12$	ΔS^+_{CPT}	$0.16 \pm 0.21 \pm 0.09$
	$C^-_{\ell^+,K^0_L}$	$0.16 \pm 0.13 \pm 0.06$	ΔC^+_{CPT}	$0.14 \pm 0.15 \pm 0.07$
(g) $B^0 \to B_-$	$S^+_{\ell^-,K^0_S}$	$-0.76 \pm 0.06 \pm 0.04$	ΔS^+_{CP}	$-1.30 \pm 0.11 \pm 0.07$
	$C^+_{\ell^-,K^0_S}$	$0.08 \pm 0.06 \pm 0.06$	ΔC^+_{CP}	$0.07 \pm 0.09 \pm 0.03$

contours calculated from the change $-2\Delta \ln \mathcal{L}$ in two dimensions for the T-asymmetry parameters $(\Delta S^+_T, \Delta C^+_T)$ and $(\Delta S^-_T, \Delta C^-_T)$. In the two cases cases we can observe that the T invariance point is excluded at 6σ level. The difference $-2\Delta \ln \mathcal{L}$ for fits assuming CPT or CP symmetry are 5 and 307, corresponding to 0.3σ and 17σ, consistent with CPT invariance and CP violation, respectively. These values, combined with those in Table II, are compatible with CP violation as due to time-reversal violation and CPT invariance. The larger significance of CP violation is because the comparison of probabilities for event classes e.g. $(\ell^- \overline{X}, c\bar{c}K^0_S)$ and $(\ell^+ X, c\bar{c}K^0_S)$ has a higher statistical and systematic significance than the comparison of e.g. $(\ell^- \overline{X}, c\bar{c}K^0_S)$ and $(\ell^- \overline{X}, c\bar{c}K^0_L)$.

Following the discussion in Sec. IV A and assuming CP conservation in mixing (i.e CP with T invariance, and CP with CPT symmetry in mixing), all eight pairs of coefficients $S^{\pm}_{\alpha,\beta}$ and $C^{\pm}_{\alpha,\beta}$ are related,

$$
\begin{aligned}
S = \ & S^+_{\ell^+,K^0_S} = -S^+_{\ell^-,K^0_S} = -S^-_{\ell^+,K^0_S} = S^-_{\ell^-,K^0_S} = \\
& -S^+_{\ell^+,K^0_L} = S^+_{\ell^-,K^0_L} = S^-_{\ell^+,K^0_L} = -S^-_{\ell^-,K^0_L}, \\
C = \ & C^+_{\ell^+,K^0_S} = -C^+_{\ell^-,K^0_S} = C^-_{\ell^+,K^0_S} = -C^-_{\ell^-,K^0_S} = \\
& C^+_{\ell^+,K^0_L} = -C^+_{\ell^-,K^0_L} = C^-_{\ell^+,K^0_L} = -C^-_{\ell^-,K^0_L}. \quad (30)
\end{aligned}
$$

In the SM, the eight $S^{\pm}_{\alpha,\beta}$ coefficients are measurements of $S = \sin 2\beta \approx 0.7$. The results in Table II lead to a mean value $S = 0.686 \pm 0.029$, which is consistent with the value obtained from the CP violation investigation based on the same data[64]. Analogously, the measurement of the eight $C^{\pm}_{\alpha,\beta}$ coefficients result in a mean value of 0.022 ± 0.021, consistent with both the previous CP analysis and zero.
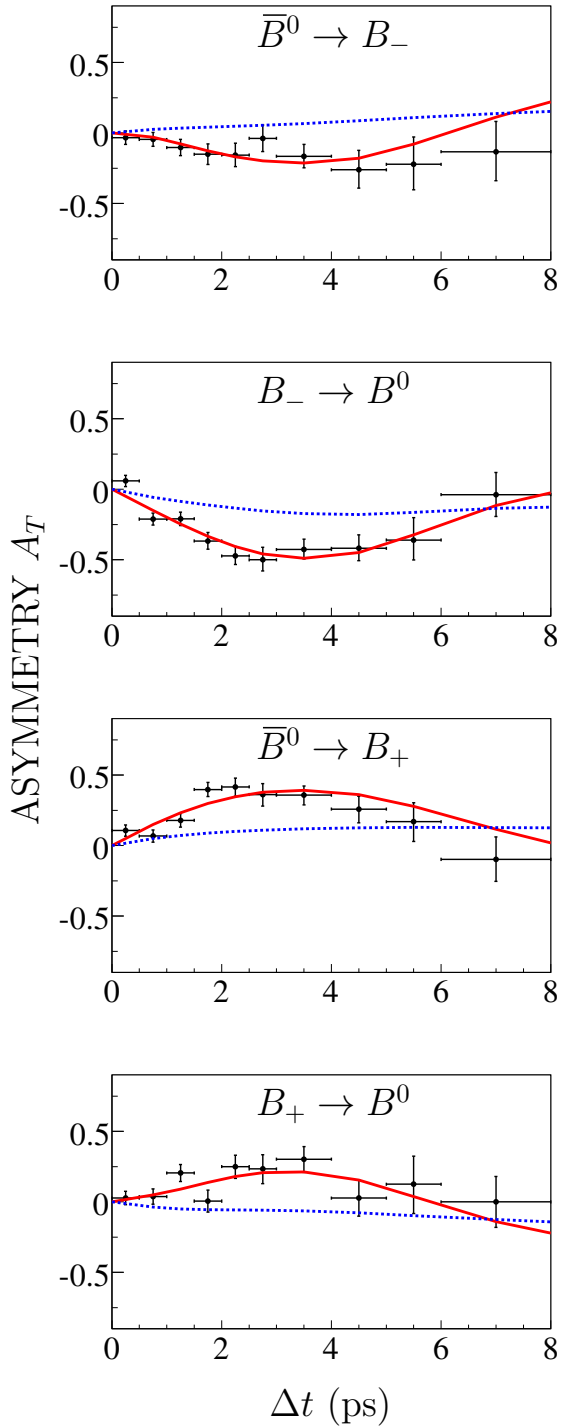
FIG. 17. The four independent asymmetries measured by the BABAR experiment[1] between transitions (from top to bottom) $\overline{B}^0 \to B_-$, $B_- \to B^0$, $\overline{B}^0 \to B_+$, $B_+ \to B^0$, and their time-reversed versions. The points with error bars represent the data, the red solid and dashed blue curves represent the projections of the best fit results with and without time-reversal violation, respectively.
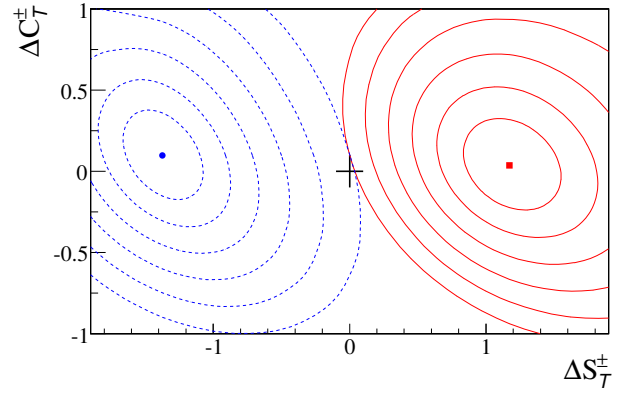

FIG. 18. Central values (blue point and red square) and two-dimensional p-value contours (for $p = 0.317$, 4.55×10^{-2}, 2.7×10^{-3}, 6.3×10^{-5}, 5.7×10^{-7}, and 2.0×10^{-9}) for the T-asymmetry parameters $(\Delta S_T^+, \Delta C_T^+)$ (blue dashed curves) and $(\Delta S_T^-, \Delta C_T^-)$ (red solid curves), as reported by BABAR[1]. The T-invariance point is shown as a $+$ sign.

VI.   CONCLUSION

The arrow of time in systems with large number of degrees of freedom is a thermodynamic property of entropy associated to the irreversibility of boundary conditions. However, time's arrow is not related to the question of time-reversal symmetry in the fundamental laws of physics. Only two physical systems in nature, the unstable K and B mesons, have a relatively large expected breaking of time-reversal symmetry; in these systems CP violation has been observed and no experimental data contradicts the CPT theorem. Therefore, K and B mesons are a best choice for an experiment detecting directly time-reversal non-invariance.

The main principle for a direct detection of time-reversal violation in transitions is the exchange of initial and final states. A unique opportunity arises from the quantum-mechanical properties imposed by the EPR entanglement between the two neutral B mesons produced in the $\Upsilon(4S)$ resonance decay at B factories. The observation of the first B decaying into the flavor eigenstates $\ell^+ X$ or $\ell^- \overline{X}$, or the CP eigenstates $c\bar{c}K_S^0$ or $J/\psi K_L^0$, prepares (tags) the initial state of the other B as $\overline{B}^0$, B^0, B_+, or B_-, respectively. The initial states tagged by entanglement are filtered at a later time through its decay into a CP- or a flavor-eigenstate decay mode. The four B meson states appearing as initial and final states make possible to build eight different transition probabilities for the time evolution of the neutral B meson. In appropriate combinations, time-reversal, CP, and CPT symmetries can be analyzed separately through four time-dependent asymmetries, which can be expressed in terms of certain asymmetry parameters.

The BABAR experiment has measured the four time-reversal asymmetries and extracted the corresponding

asymmetry parameters. The results show a highly significant departure from motion reversal symmetry. A precise exchange of initial and final states is needed to interpret the results as direct detection of time-reversal non-invariance. This requires the absence of both wrong-strangeness ($B^0 \nrightarrow c\bar{c}\bar{K}^0$ and $\bar{B}^0 \nrightarrow c\bar{c}K^0$) and wrong-sign ($B^0 \nrightarrow \ell^- \bar{X}$ and $\bar{B}^0 \nrightarrow \ell^+ X$) B decays, CP invariance in K^0-$\bar{K}^0$ mixing, and $|\bar{A}/A| = 1$ (a single decay amplitude and CPT symmetry in the $B^0 \to c\bar{c}K^0$ decay amplitude). All these effects are small and have been either accounted for in the systematic uncertainties (the second), directly demonstrated in the experimental analysis and incorporated in the uncertainties (the fourth), or neglected since their impact is well below the statistical sensitivity [$\mathcal{O}(10\%)$] according to measurements [the first, $\mathcal{O}(0.1\%)$] or SM expectations [the third, $\mathcal{O}(1\%)$].

Time-reversal and CP symmetry breakings are seen in two separate observations (the states involved in the transitions are not CP conjugate to each other) and the asymmetries are time dependent with only a $\sin(\Delta m_d \Delta t)$ term, of order $\mathcal{O}(10^{-1})$, and are induced by the interference of decay amplitudes with and without mixing. The corresponding measurement of the weak phase from time-reversal asymmetries match those from CP asymmetries, therefore the observed T and CP violations balance to each other, supporting CPT invariance in the time evolution of B mesons. This is in contrast to the flavor-mixing asymmetry in K^0-$\bar{K}^0$ transitions measured by CPLEAR, where CP and T transformations are identical and the asymmetry is time independent, of order $\mathcal{O}(10^{-3})$, and is produced by the interference between the dispersive and absorptive contributions to K^0-$\bar{K}^0$ mixing.

The concept of direct detection of time-reversal violation in transitions might be extended to include systematic tests using pairs of B and D mesons created in the decay of the $\Upsilon(4S)$ and $\psi(3770)$ resonances[80], as well as pairs of K mesons from the $\phi(1020)$[81]. In the latter case, there are important differences triggered by a non-vanishing decay width difference, the non-orthogonality of the K_L^0 and K_S^0 states, and the small effects expected within the SM. This opens the possibility to embark upon a complete time-reversal (and CPT) violation program in weak interactions to probe possible new physics contributions in tree and loop decays at future high-luminosity flavor factories, Belle II at SuperKEKB[82,83] and KLOE-2 at DAΦNE[84].

The main limitation of the method is associated with the identification of the appropriate decay channels used to filter the states of the time-reversed transition. Specifically, it is necessary to identify pairs of decay channels that project into meson states orthogonal to each other This orthogonality condition is satisfied by conjugate flavor eigenstate decay channels ($\ell^- \bar{X}, \ell^+ X$) and by CP eigenstates of opposite CP parity with the same flavor content ($c\bar{c}K_S^0, J/\psi K_L^0$). The fact that the B decay amplitudes to $c\bar{c}K_S^0$ and $J/\psi K_L^0$ are given by the same diagram followed by K^0-$\bar{K}^0$ mixing (needed to make possible the interference) is essential for the definition of the states B_- and B_+. The precise implementation of these restrictions imposes the requirements summarized above. An alternative time-reversal asymmetry based on EPR entanglement open to any pair of decay channels has been recently suggested[85], though the connection between the experiment and the time-reversal observables requires some theoretical input.

[1] J. P. Lees *et al.* (*BABAR* Collaboration), Phys.Rev.Lett. **109**, 211801 (2012).
[2] M. Zeller, "Particle decays point to an arrow of time," Physics **5**, 129 (2012).
[3] B. M. Schwarzschild, "Time-reversal asymmetry in particle physics has finally been clearly seen," Phys. Today **65(11)**, 16 (2012).
[4] "Time's arrow in B mesons," Nature **491**, 640 (2012).
[5] "*BABAR* makes first direct measurement of time-reversal violation," Physics World, November **11** (2012).
[6] "Physics World reveals its top 10 breakthroughs for 2012," Physics World, December **12** (2012).
[7] "The arrow of time. Backward ran sentences...." The Economist, September 1st, 60(2012).
[8] J. H. Christenson, J. W. Cronin, V. L. Fitch, and R. Turlay, Phys.Rev.Lett. **13**, 138 (1964).
[9] J. H. Christenson, J. W. Cronin, V. L. Fitch, and R. Turlay, Phys.Rev. **140**, B74 (1965).
[10] B. Aubert *et al.* (*BABAR* Collaboration), Phys.Rev.Lett. **87**, 091801 (2001).
[11] K. Abe *et al.* (Belle Collaboration), Phys.Rev.Lett. **87**, 091802 (2001).
[12] M. C. Banuls and J. Bernabeu, Phys.Lett.B **464**, 117 (1999).
[13] M. C. Banuls and J. Bernabeu, Nucl.Phys.B **590**, 19 (2000).
[14] L. Wolfenstein, Int.J.Mod.Phys.E **8**, 501 (1999).
[15] E. P. Wigner, Nachr. Ges. Wiss. Göttingen **32**, 35 (1932).
[16] E. M. Henley, Int.J.Mod.Phys.E **22**, 1330010 (2013).
[17] R. G. Sachs, "The Physics of Time Reversal," The University of Chicago Press, 1–325(1987).
[18] T. D. Lee, "Particle physics and introduction to field theory," Hardwood, Chur, 1–881(1990).
[19] G. C. Branco, L. Lavoura, and J. P. Silva, "CP Violation," Int.Ser.Monogr.Phys. **103**, 1–536 (1999).
[20] E. Blanke, H. Driller, W. Glockle, H. Genz, A. Richter, *et al.*, Phys.Rev.Lett. **51**, 355 (1983).
[21] A. S. Eddington, "The nature of the physical world," Nabu Press, 1–390(2011).
[22] A. H. Guth, Phys.Rev.D **23**, 347 (1981).
[23] A. H. Guth and S. Y. Pi, Phys.Rev.Lett. **49**, 1110 (1982).
[24] P. A. R. Ade *et al.* (Planck Collaboration), "Planck 2013 results. I. Overview of products and scientific results," Astronomy & Astrophysics manuscript no. PlanckMission2013(2013).
[25] P.A.R. Ade *et al.* (BICEP2 Collaboration), "BICEP2 I: Detection Of B-mode Polarization at Degree Angular Scales," (2014), arXiv:1403.3985.

[26]T. D. Lee and C.-N. Yang, Phys.Rev. **104**, 254 (1956).

[27]C. S. Wu, E. Ambler, R. W. Hayward, D. D. Hoppes, and R. P. Hudson, Phys.Rev. **105**, 1413 (1957).

[28]R. L. Garwin, L. M. Lederman, and M. Weinrich, Phys.Rev. **105**, 1415 (1957).

[29]N. Cabibbo, Phys.Rev.Lett. **10**, 531 (1963).

[30]M. Kobayashi and T. Maskawa, Prog.Theor.Phys. **49**, 652 (1973).

[31]J. Beringer *et al.* (Particle Data Group), Phys.Rev.D **86**, 010001 (2012).

[32]L. Wolfenstein, Phys.Rev.Lett. **51**, 1945 (1983).

[33]M. Antonelli, D. M. Asner, D. A. Bauer, T. G. Becher, M. Beneke, *et al.*, Phys.Rept. **494**, 197 (2010).

[34]M. Perl *et al.*, Phys.Rev.Lett. **35**, 1489 (1975).

[35]S. W. Herb *et al.*, Phys.Rev.Lett. **39**, 252 (1977).

[36]G. Lüders, Annals Phys. **2**, 1 (1957).

[37]W. Pauli, L. Rosenfold, and V. Weisskopf, "Niels Bohr and the development of Physics," Pergamon Press NY(1995).

[38]R. D. Peccei and H. R. Quinn, Phys.Rev.Lett. **38**, 1440 (1977).

[39]M. Gronau and J. L. Rosner, Phys.Rev. **D84**, 096013 (2011).

[40]N. Cabibbo, Phys.Lett.B **72**, 333 (1978).

[41]B. Aubert *et al.* (*BABAR* Collaboration), Phys.Rev.Lett. **93**, 131801 (2004).

[42]Y. Chao *et al.* (Belle Collaboration), Phys.Rev.Lett. **93**, 191802 (2004).

[43]J. Bernabeu and C. Jarlskog, Z.Phys.C **8**, 233 (1981).

[44]The proof is as follows: if $A_1 = a_1 \exp[i(\delta_1 + \phi_1)]$ and $A_2 = a_2 \exp[i(\delta_2 + \phi_2)]$ are the two possible amplitudes for the process $i \to f$, with a_1 and a_2 real numbers, and $\bar{i}$ and $\bar{f}$ are the *CP*-conjugate states of i and f, respectively, then $|A(i \to f)|^2 - |A(\bar{i} \to \bar{f})|^2 = -4a_1 a_2 \sin(\Delta\delta) \sin(\Delta\phi)$ do not vanish only if both $\Delta\delta$ and $\Delta\phi$ are non-vanishing.

[45]P. K. Kabir, Phys.Rev.D **2**, 540 (1970).

[46]I. I. Bigi and A. I. Sanda, "*CP* violation," Camb. Monogr. Part. Phys. Nucl. Phys. Cosmol. **9**, 1–382 (2000).

[47]A. Angelopoulos *et al.* (CPLEAR Collaboration), Phys.Lett.B **444**, 43 (1998).

[48]V. Weisskopf and E. P. Wigner, Z.Phys. **63**, 54 (1930).

[49]V. Weisskopf and E. P. Wigner, Z.Phys. **65**, 18 (1930).

[50]L. Wolfenstein, Phys.Rev.Lett. **83**, 911 (1999).

[51]J. P. Lees *et al.* (*BABAR* Collaboration), Phys.Rev.Lett. **111**, 101802 (2013).

[52]V. M. Abazov *et al.* (D0 Collaboration), Phys.Rev.D **86**, 072009 (2012).

[53]B. Aubert *et al.* (*BABAR* Collaboration), Phys.Rev.Lett. **96**, 251802 (2006).

[54]E. Nakano *et al.* (Belle Collaboration), Phys.Rev.D **73**, 112002 (2006).

[55]L. Alvarez-Gaume, C. Kounnas, S. Lola, and P. Pavlopoulos, Phys.Lett.B **458**, 347 (1999).

[56]J. R. Ellis and N. E. Mavromatos, Phys.Rept. **320**, 341 (1999).

[57]H. J. Gerber, Eur.Phys.J.C **35**, 195 (2004).

[58]B. Aubert *et al.* (*BABAR* Collaboration), Nucl.Instrum.Meth.A, 615(2013).

[59]B. Aubert *et al.* (*BABAR* Collaboration), Nucl.Instrum.Meth.A **479**, 1 (2002).

[60]A. Abashian *et al.*, Nucl.Instrum.Meth.A **479**, 117 (2002).

[61]H. J. Lipkin, Phys.Lett.B **219**, 474 (1989).

[62]A. Einstein, B. Podolsky, and N. Rosen, Phys.Rev. **47**, 777 (1935).

[63]M. D. Reid, P. D. Drummond, W. P. Bowen, E. G. Cavalcanti, P. K. Lam, *et al.*, Rev.Mod.Phys. **81**, 1727 (2009).

[64]B. Aubert *et al.* (*BABAR* Collaboration), Phys.Rev.D **79**, 072009 (2009).

[65]K. R. Schubert, L. Li Gioi, A. J. Bevan, and A. Di Domenico(2014), arXiv:1401.6938 [hep-ex].

[66]T. D. Lee, R. Oehme, and C.-N. Yang, Phys.Rev. **106**, 340 (1957).

[67]C. P. Enz and R. R. Lewis, Helv.Phys.Acta **38**, 860 (1965).

[68]H. Boos, T. Mannel, and J. Reuter, Phys.Rev.D **70**, 036006 (2004).

[69]H. Boos, T. Mannel, and J. Reuter, JHEP **0703**, 009 (2007).

[70]C.-W. Chiang, A. Datta, M. Duraisamy, D. London, M. Nagashima, *et al.*, JHEP **1004**, 031 (2010).

[71]B. Aubert *et al.* (*BABAR* Collaboration), Phys.Rev.Lett. **92**, 181801 (2004).

[72]B. Aubert *et al.* (*BABAR* Collaboration), Phys.Rev. **D70**, 012007 (2004).

[73]M. Fidecaro, H.-J. Gerber, and T. Ruf(2013), arXiv:1312.3770 [hep-ph].

[74]H. R. Quinn, J.Phys.Conf.Ser. **171**, 011001 (2009).

[75]J. Bernabeu, F. Martinez-Vidal, and P. Villanueva-Perez, JHEP **1208**, 064 (2012).

[76]The K_L^0 state is experimentally found to be the heavier state.

[77]M. C. Banuls and J. Bernabeu, JHEP **9906**, 032 (1999).

[78]E. Applebaum, A. Efrati, Y. Grossman, Y. Nir, and Y. Soreq, Phys.Rev.D **89**, 076011 (2014).

[79]Eight is the difference in the number of fit constraints with and without T violation.

[80]A. J. Bevan, G. Inguglia, and M. Zoccali(2013), arXiv:1302.4191 [hep-ph].

[81]J. Bernabeu, A. Di Domenico, and P. Villanueva-Perez, Nucl.Phys.B **868**, 102 (2013).

[82]T. Abe *et al.* (Belle II Collaboration)(2010), arXiv:1011.0352 [physics.ins-det].

[83]T. Aushev, W. Bartel, A. Bondar, J. Brodzicka, T. E. Browder, *et al.*(2010), arXiv:1002.5012 [hep-ex].

[84]G. Amelino-Camelia, F. Archilli, D. Babusci, D. Badoni, G. Bencivenni, *et al.*, Eur.Phys.J.C **68**, 619 (2010).

[85]J. Bernabeu, F. J. Botella, and M. Nebot, Phys.Lett.B **728**, 95 (2014).